Available online at www.sciencedirect.com
ScienceDirect
Journal of Sound and Vibration 325 (2009) 397–420
JOURNAL OF SOUND AND VIBRATION
www.elsevier.com/locate/jsvi

Modal properties of three-dimensional helical planetary gears

Tugan Eritenel, Robert G. Parker*

Department of Mechanical Engineering, The Ohio State University, 201 W. 19th Ave. Columbus, OH 43210, USA

Received 27 October 2008; received in revised form 1 March 2009; accepted 2 March 2009
Handling Editor: L.G. Tham
Available online 10 April 2009

Abstract

The structured modal properties of single-stage helical planetary gears with equally spaced planets are categorized and mathematically proved. Compared to prior two-dimensional analyses of spur gears, this study examines the three-dimensional motion of the helical gears and shafts. A lumped-parameter model is formulated to obtain the equations of motion. The gear-shaft bodies are modeled as rigid bodies with compliant bearings at arbitrary axial locations on the shafts. A translational and a tilting stiffness account for the force and moment transmission at the gear mesh interface. The derived modal properties generalize those of two-dimensional spur planetary gears; there are twice as many degrees of freedom and natural frequencies due to the added tilting and axial motion. All vibration modes are categorized as rotational–axial, translational–tilting, and planet modes. The modal properties are shown to hold even for configurations that are not symmetric about the gear plane, due to, for example, shaft bearings not being equidistant from the gear plane.

1. Introduction

Knowledge of the modal properties of planetary gears is crucial for developing strategies to reduce vibration. Planetary gear dynamic models are developed in Refs. [1–4]. Lin and Parker show that two-dimensional, spur planetary gears with equally spaced [5] and diametrically opposed [6] planets possess well-defined modal properties. They report all vibration modes belong to one of the three categories: (1) Rotational modes where the central members (sun, carrier, and ring) rotate but do not translate. The planet motions are identical. (2) Translational modes with degenerate natural frequencies, where the central members translate but do not rotate. There are well-defined relations between the two independent vibration modes at each natural frequency. (3) Planet modes where only the planets move, and their motions are scalar multiples of the arbitrarily chosen first planet's motion. Kiracofe and Parker [7] prove that a similar categorization applies to compound planetary gears. Wu and Parker [8] prove the modal properties of spur planetary gears having elastically deformable ring gears.

These vibration mode characteristics are crucial in vibration suppression strategies using mesh phasing [2,9,10] and eigensensitivity analysis [11,12] of planetary gears. Schlegel and Mard [10], Seager [2], and Hidaka et al. [13] assert that the vibration of planetary gears is reduced by proper gear mesh phasing. Hidaka et al. [13] experimentally and Kahraman [14] computationally investigate the effectiveness of vibration suppression by

*Corresponding author. Tel.: +1 614 688 3922; fax: +1 614 292 3163.
E-mail address: parker.242@osu.edu (R.G. Parker).

0022-460X/$ - see front matter
doi:10.1016/j.jsv.2009.03.002

Nomenclature

c_j	axial position of the center of stiffness at the jth mesh
e_b	axial position of the center of mass of body b
J_b^x	tilting moment of inertia of body b
J_b^z	polar moment of inertia of body b
k_b^A	translational stiffness of bearing A on body b
k_b^{Az}	axial stiffness of bearing A on body b
k_b^B, k_b^{Bz}	analogous definitions for bearing B as for bearing A
k_j	translational gear mesh stiffness at the jth mesh
L_b^A	axial position of bearing A on body b
L_b^B	axial position of bearing B on body b
m_b	mass of body b
p	number of planets
r_b	base radius of gear b
x_b, y_b, z_b	translational deflections of body b along $\mathbf{E}_1$, $\mathbf{E}_2$, and $\mathbf{E}_3$
α_i	angular position of the ith planet
ϕ_b, θ_b, β_b	angular deflections of body b about $\mathbf{E}_1$, $\mathbf{E}_2$, and $\mathbf{E}_3$
Φ_{sp}	transverse operating pressure angle of sun–planet meshes
Φ_{rp}	transverse operating pressure angle of ring–planet meshes
κ_b^A	tilting stiffness of bearing A on body b
κ_b^{Az}	axial rotation stiffness of bearing A on body b
κ_b^B, κ_b^{Bz}	analogous definitions for bearing B as for bearing A
κ_j	tilting gear mesh stiffness at the jth mesh
Ω_b	rotation speed of body b
ψ	base helix angle

Subscripts

b	body index, $b = s, r, c, 1, \ldots, p$
c	carrier
h	central member index, $h = s, r, c$
i	planet index, $i = 1, 2, \ldots, p$
j	gear mesh index (odd are sun–planet, even are ring–planet meshes)
r	ring gear
s	sun gear

planet mesh phasing. Kahraman [14] uses a three-dimensional lumped-parameter model for computations. Blankenship and Kahraman [15] illustrate how some harmonics of the transmission error excitation vanish by adjusting the mesh phasing. Based on the well-defined modal properties of planetary gears, Parker [16] explains how proper mesh phasing suppresses many resonances of translational and rotational modes from certain harmonics of mesh frequency. Ambarisha and Parker [17] explain the vibration suppression of planet modes from mesh phasing.

Finite element analysis is incorporated with elaborate gear contact analysis in Refs. [18–21] to capture the complex dynamic behavior of planetary gears. These studies enable computationally efficient analysis of complex planetary gears and survey the effects of design parameters on dynamic behavior.

Although the vibration modes of two-dimensional planetary gears have been studied, it remains to be seen what the vibration mode characteristics are for helical planetary gears with three-dimensional motion, a three-dimensional gear mesh interface, and the gear-shaft bodies supported by bearings at arbitrary locations along the shafts. A lumped-parameter model is formulated to include the tilting and axial motions, thus including all six degrees of freedom for each gear-shaft body. A tilting mesh stiffness augments the gear mesh interface to produce the three-dimensional force and moment transmission.

This study proves that helical planetary gears with equally spaced planets have exactly three types of vibration modes. Unique properties of these vibration modes are given. Compared to two-dimensional spur gear models there are twice as many natural modes, and their properties are different. The modal properties hold for configurations that are asymmetric about the gear plane, such as when the bearings are not equidistant from the gears.

2. Planetary gear analytical model

The planetary gear model consists of three central members (the sun, ring, and carrier) and p planets. The gears and the carrier are integrated with their supporting shafts, so that each gear-shaft is a single body.

These combined gear-shaft bodies are each mounted on up to two bearings placed at arbitrary axial locations. The sun, ring, and carrier bearings are connected to ground while the planet bearings are connected to the carrier. The gear-shaft bodies and carrier are rigid; the compliant elements are the meshing gear teeth and bearings. Figs. 1(a) and (b) depict the model with the parameters defining the system geometry. The vibration amplitudes are small, so geometric nonlinearities are neglected.

The indexing conventions $b = s, r, c, 1, \ldots, p$ for the sun, ring, carrier, and the planets, $h = s, r, c$ for the sun, ring, and carrier, and $i = 1, 2, \ldots, p$ for the planets are maintained throughout this work. There are $2p$ gear meshes. Odd numbers are assigned to the sun–planet meshes, and even numbers are assigned to the ring–planet meshes.

The origin is at the undeflected position of the center of the sun. A right handed, orthonormal basis $\{\mathbf{E}\} = \{\mathbf{E}_1, \mathbf{E}_2, \mathbf{E}_3\}$ rotates with the constant carrier angular speed Ω_c. For the central members, translational coordinates x_h, y_h, z_h are assigned to translations along $\mathbf{E}_1$, $\mathbf{E}_2$, and $\mathbf{E}_3$, respectively. Similarly, angular coordinates ϕ_h, θ_h, β_h are assigned to small rotations about $\mathbf{E}_1$, $\mathbf{E}_2$, and $\mathbf{E}_3$, respectively. Translational coordinates for the planets x_i, y_i, z_i are measured from the undeflected position of the centers of the planets in the bases $\{\mathbf{E}^i\} = \{\mathbf{E}_1^i, \mathbf{E}_2^i, \mathbf{E}_3^i\}$ that rotate with the carrier angular speed. The base vector $\mathbf{E}_1^i$ is parallel to the line of action of the ith sun–planet mesh because this selection algebraically simplifies the sun–planet mesh deflections. Angular coordinates ϕ_i, θ_i, β_i for

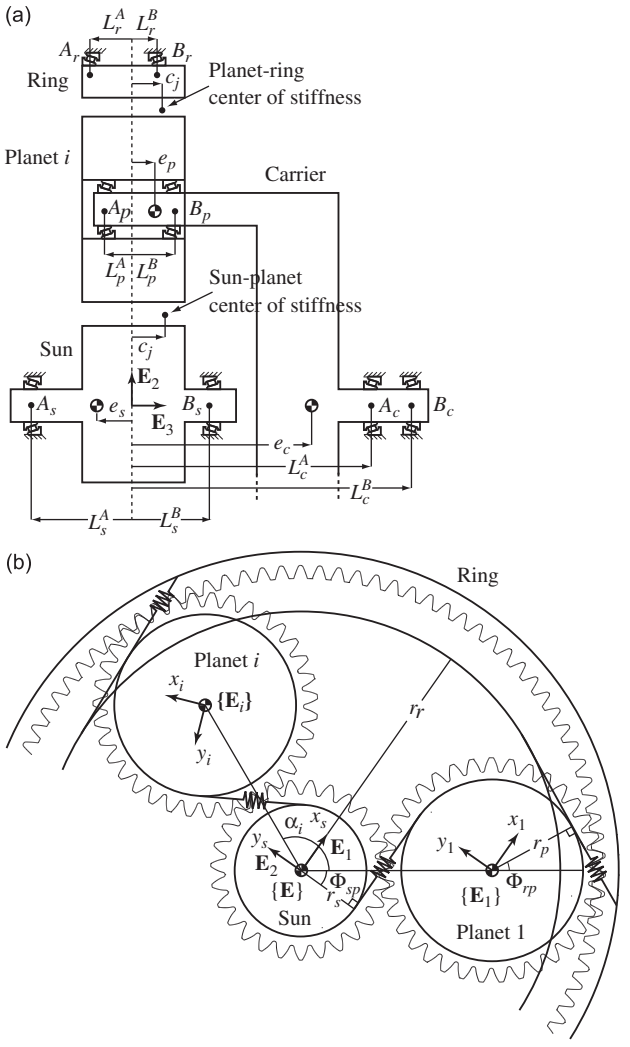

Fig. 1. Coordinates and dimensions used in the planetary gear model. The parameters are defined in Nomenclature.

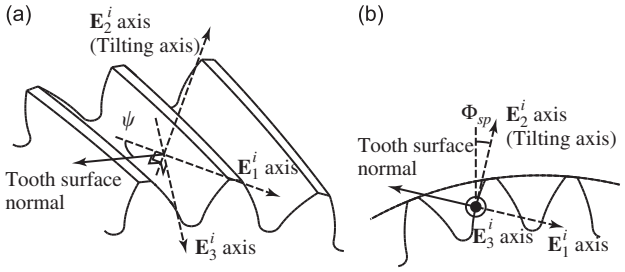

Fig. 2. Tooth surface normal and the tilting axis for the ith sun–planet mesh. The ith planet gear is shown. ψ is the base helix angle, and Φ_{sp} is the transverse operating pressure angle.

the planets are assigned to rotations about $\mathbf{E}_1^i$, $\mathbf{E}_2^i$, and $\mathbf{E}_3^i$, respectively. Body fixed bases for all the bodies $\{\mathbf{e}^b\} = \{\mathbf{e}_1^b, \mathbf{e}_2^b, \mathbf{e}_3^b\}$ are adopted because the gear mesh deflection expressions are algebraically simpler in these bases.

Axial position quantities in Fig. 1(a) are measured from the datum position, which is at the center of the minimum active facewidth F and denoted by the dashed line. Any inactive facewidth is considered as part of the shaft. This setup allows arbitrary axial positioning of gears with different facewidths. Positive planet position angle α_i is measured counter-clockwise from the arbitrarily chosen first planet.

Two linear springs, one translational and one tilting, model the gear mesh interface. The translational stiffness (k_j) accounts for the transmitted force through the gear mesh. Its associated relative translational deflection (δ_j) is in the direction of the tooth surface normal. The tilting stiffness (κ_j) accounts for the moment transmitted through the gear mesh. Its associated angular deflection is about an axis that is in the gear plane and perpendicular to both the line of action $\mathbf{E}_1^i$ and the tooth surface normal. Fig. 2 shows the line of action $\mathbf{E}_1^i$, the tooth surface normal, and the tilting axis $\mathbf{E}_2^i$ for the ith sun–planet mesh. These two deflections are calculated at a specified point along the facewidth, called the center of stiffness. The axial position of the center of stiffness is c_j. The translational stiffness, tilting stiffness, and center of stiffness can be reduced from gear tooth contact models, such as Ref. [22], averaged over a mesh cycle.

The equations of motion come from Lagrange's equations for unconstrained generalized coordinates. The kinetic and potential energies are

$$T = \frac{1}{2}\sum_{b=1}^{N}(\boldsymbol{\omega}_b^{\mathrm{T}}\mathbf{J}_b\boldsymbol{\omega}_b + \dot{\mathbf{r}}_b^{\mathrm{T}}m_b\dot{\mathbf{r}}_b),$$

$$V = \frac{1}{2}\sum_{b=1}^{N}(\mathbf{d}_{A,b}^{\mathrm{T}}\mathbf{K}_{A,b}\mathbf{d}_{A,b} + \mathbf{d}_{B,b}^{\mathrm{T}}\mathbf{K}_{B,b}\mathbf{d}_{B,b}) + \frac{1}{2}\sum_{b=1}^{N}(\boldsymbol{\zeta}_{A,b}^{\mathrm{T}}\boldsymbol{\chi}_{A,b}\boldsymbol{\zeta}_{A,b} + \boldsymbol{\zeta}_{B,b}^{\mathrm{T}}\boldsymbol{\chi}_{B,b}\boldsymbol{\zeta}_{B,b}) + \frac{1}{2}\sum_{j=1}^{2p}(k_j\delta_j^2 + \kappa_j\gamma_j^2), \tag{1}$$

where $N = p + 3$ is the number of bodies, $\boldsymbol{\omega}_b$ is the angular velocity, m_b is the mass, $\mathbf{J}_b$ is the inertia tensor, $\dot{\mathbf{r}}_b$ is the velocity vector, $\mathbf{d}_{A,b}$ is the translational bearing deflection vector, $\boldsymbol{\zeta}_{A,b}$ is the angular bearing deflection vector, $\mathbf{K}_{A,b}$ is the bearing stiffness matrix for translation, and $\boldsymbol{\chi}_{A,b}$ is the bearing stiffness matrix for rotation. The translational gear mesh deflection is δ_j; the angular (tilting) gear mesh deflection is γ_j; the translational gear mesh stiffness is k_j; and the tilting gear mesh stiffness is κ_j.

The angular velocity of the bth body in its corotational basis $\{\mathbf{e}^b\}$ is

$$\boldsymbol{\omega}_b = [\dot{\phi}_b - \theta_b(\dot{\beta}_b + \Omega_b)]\mathbf{e}_1^b + [\dot{\theta}_b + \phi_b(\dot{\beta}_b + \Omega_b)]\mathbf{e}_2^b + [\dot{\beta}_b + \Omega_b - \phi_b\dot{\theta}_b]\mathbf{e}_3^b, \tag{2}$$

where Ω_b is the constant kinematic rotation speed. The inertia tensor for each body in its principal axes is $\mathbf{J}_b = \mathrm{diag}[J_b^x, J_b^y, J_b^z]$ with constant components. All gears are axisymmetric, so $J_b^y = J_b^x$. The velocity vectors of the central members and planets are

$$\dot{\mathbf{r}}_h = [\dot{x}_h - \Omega_c y_h]\mathbf{E}_1 + [\dot{y}_h + \Omega_c x_h]\mathbf{E}_2 + \dot{z}_h\mathbf{E}_3, \quad h = s, r, c, \tag{3}$$

$$\dot{\mathbf{r}}_i = [\dot{x}_h - \Omega_c(y_i - r_s - r_p)]\mathbf{E}_1^i + [\dot{y}_i + \Omega_c(x_i + \tan\Phi_{\mathrm{sp}}(r_s + r_p))]\mathbf{E}_2^i + \dot{z}_i\mathbf{E}_3^i, \quad i = 1, 2, \ldots, p, \tag{4}$$

where Φ_{sp} and Φ_{rp} are the sun–planet and ring–planet transverse operating pressure angles.

The bearings are attached to the points A_b and B_b on the left and right sides of the bth body, respectively. The bearing deflection vectors for central members at points A_h and B_h ($h = s, r, c$) are

$$\mathbf{d}_{A,h} = [x_h - (e_h + L_h^A)\theta_h]\mathbf{E}_1 + [(e_h + L_h^A)\phi_h + y_h]\mathbf{E}_2 + z_h\mathbf{E}_3, \tag{5}$$

$$\mathbf{d}_{B,h} = [x_h - (e_h - L_h^B)\theta_h]\mathbf{E}_1 + [(e_h - L_h^B)\phi_h + y_h]\mathbf{E}_2 + z_h\mathbf{E}_3, \tag{6}$$

where e_h, L_h^A, and L_h^B are the axial positions of the mass centers, bearings A_h, and bearings B_h of the central members. Positive values of e_h and L_b^A are measured from the datum along $\mathbf{E}_3$, and positive values of L_b^B are measured from the datum along $-\mathbf{E}_3$. This sign convention is chosen so that for positive L_b^A and L_b^B the gears are in between the bearings. The bearing deflection vector for the planets is the relative position between the point that is on the carrier and the point that is on the planet shaft. The bearing deflection vectors for the planets at points A_i and B_i are

$$\begin{aligned}\mathbf{d}_{A,i} = {} & \{-[y_c + \phi_c(e_s + L_p^A)]\sin\alpha_i + [\theta_c(e_s + L_p^A) - x_c]\cos\alpha_i - \beta_c(r_p + r_s) + x_i - \theta_i(e_p + L_p^A)\}\mathbf{E}_1^i \\ & + \{[x_c - \theta_c(e_s + L_p^A)]\sin\alpha_i - [y_c + \phi_c(e_s + L_p^A)]\cos\alpha_i - \beta_c(r_p + r_s)\tan\Phi_{\mathrm{sp}} + y_i + \phi_i(e_p + L_p^A)\}\mathbf{E}_2^i \\ & + \{[-\phi_c(r_s + r_p)\tan\Phi_{\mathrm{sp}} + \theta_c(r_s + r_p)]\sin\alpha_i + [\theta_c(r_s + r_p)\tan\Phi_{\mathrm{sp}} + \phi_c(r_s + r_p)]\cos\alpha_i + z_i - z_c\}\mathbf{E}_3^i,\end{aligned} \tag{7}$$

$$\begin{aligned}\mathbf{d}_{B,i} = {} & \{-[y_c + \phi_c(e_s - L_p^B)]\sin\alpha_i + [\theta_c(e_s - L_p^B) - x_c]\cos\alpha_i - \beta_c(r_p + r_s) + x_i - \theta_i(e_p - L_p^B)\}\mathbf{E}_1^i \\ & + \{[x_c - \theta_c(e_s - L_p^B)]\sin\alpha_i - [y_c + \phi_c(e_s - L_p^B)]\cos\alpha_i - \beta_c(r_p + r_s)\tan\Phi_{\mathrm{sp}} + y_i + \phi_i(e_p - L_p^B)\}\mathbf{E}_2^i \\ & + \{[-\phi_c(r_s + r_p)\tan\Phi_{\mathrm{sp}} + \theta_c(r_s + r_p)]\sin\alpha_i + [\theta_c(r_s + r_p)\tan\Phi_{\mathrm{sp}} + \phi_c(r_s + r_p)]\cos\alpha_i + z_i - z_c\}\mathbf{E}_3^i.\end{aligned} \tag{8}$$

The angular bearing deflection vector is the relative angular displacements of the connected bodies. The angular bearing deflection vectors for the central members and planets at points A_h and A_i are

$$\boldsymbol{\zeta}_{A,h} = \phi_h\mathbf{E}_1 + \theta_h\mathbf{E}_2 + \beta_h\mathbf{E}_3, \tag{9}$$

$$\boldsymbol{\zeta}_{A,i} = [\phi_i - \theta_c\sin\alpha_i - \phi_c\cos\alpha_i]\mathbf{E}_1^i + [\theta_i - \theta_c\cos\alpha_i + \phi_c\sin\alpha_i]\mathbf{E}_2^i + [\beta_i - \beta_c]\mathbf{E}_3^i. \tag{10}$$

The angular bearing deflection vectors at points B_h and B_i are identical to Eqs. (9) and (10) for rigid shafts.

The bearings are isotropic in the $\mathbf{E}_1-\mathbf{E}_2$ plane. There is no coupling between different directions. For all bodies the bearing stiffness matrix for translation is $\mathbf{K}_{A,b} = \mathrm{diag}[k_b^A, k_b^A, k_b^{Az}]$, and the bearing stiffness matrix for rotation is $\boldsymbol{\chi}_{A,b} = \mathrm{diag}[\kappa_b^A, \kappa_b^A, \kappa_b^{Az}]$, where the equality of stiffness in the two in-plane translation directions is evident (and similarly for rotation). These stiffness components are in the $\{\mathbf{E}\}$ basis for the central members and in the $\{\mathbf{E}^i\}$ basis for each of the planets.

The translational gear mesh deflection δ_j is the relative compressive deflection at the center of stiffness in the direction normal to the tooth surface. The translational gear mesh deflection for the sun–planet meshes ($j = 1, 3, 5, \ldots, 2p-1$) is

$$\begin{aligned}\delta_j = {} & \{[(e_s - c_j)\phi_s + y_s]\cos\psi + r_s[\theta_s - \phi_s\tan\Phi_{\mathrm{sp}}]\sin\psi\}\sin\alpha_i \\ & + \{[x_s - (e_s - c_j)\theta_s]\cos\psi + r_s[\phi_s + \theta_s\tan\Phi_{\mathrm{sp}}]\sin\psi\}\cos\alpha_i \\ & + [(e_p - c_j)\theta_i + r_s\beta_s + r_p\beta_i - x_i]\cos\psi + [z_i - z_s + r_p(\phi_i + \theta_i\tan\Phi_{\mathrm{sp}})]\sin\psi,\end{aligned} \tag{11}$$

where ψ is the base helix angle, and the center of stiffness for a gear mesh in the axial direction measured from the datum is c_j. For the ring–planet meshes ($j = 2, 4, \ldots, 2p$) the translational gear mesh deflection is

$$\begin{aligned}\delta_j = {} & \{r_r[(\phi_r - \theta_r\tan\Phi_{\mathrm{rp}})\sin(\Phi_{\mathrm{sp}} + \Phi_{\mathrm{rp}}) - (\theta_r + \phi_r\tan\Phi_{\mathrm{rp}})\cos(\Phi_{\mathrm{sp}} + \Phi_{\mathrm{rp}})]\sin\psi \\ & + [((e_r - c_j)\theta_r - x_r)\sin(\Phi_{\mathrm{sp}} + \Phi_{\mathrm{rp}}) + ((e_r - c_j)\phi_r + y_r)\cos(\Phi_{\mathrm{sp}} + \Phi_{\mathrm{rp}})]\cos\psi\}\sin\alpha_i \\ & - \{r_r[(\theta_r + \phi_r\tan\Phi_{\mathrm{rp}})\sin(\Phi_{\mathrm{sp}} + \Phi_{\mathrm{rp}}) + (\phi_r - \theta_r\tan\Phi_{\mathrm{rp}})\cos(\Phi_{\mathrm{sp}} + \Phi_{\mathrm{rp}})]\sin\psi \\ & + [((e_r - c_j)\phi_r + y_r)\sin(\Phi_{\mathrm{sp}} + \Phi_{\mathrm{rp}}) + ((c_j - e_r)\theta_r + x_r)\cos(\Phi_{\mathrm{sp}} + \Phi_{\mathrm{rp}})]\cos\psi\}\cos\alpha_i \\ & + \{r_p[(\phi_i - \theta_i\tan\Phi_{\mathrm{rp}})\cos(\Phi_{\mathrm{sp}} + \Phi_{\mathrm{rp}}) + (\phi_i\tan\Phi_{\mathrm{rp}} + \theta_i)\sin(\Phi_{\mathrm{sp}} + \Phi_{\mathrm{rp}})] + z_r - z_i\}\sin\psi \\ & + \{[(e_p - c_j)\theta_i - x_i]\cos(\Phi_{\mathrm{sp}} + \Phi_{\mathrm{rp}}) + [(c_j - e_p)\phi_i - y_i]\sin(\Phi_{\mathrm{sp}} + \Phi_{\mathrm{rp}}) - r_p\beta_i\}\cos\psi.\end{aligned} \tag{12}$$

The angular gear mesh deflection γ_j for the sun–planet and ring–planet meshes is

$$\gamma_j = \phi_s \sin\alpha_i - \theta_s \cos\alpha_i + \theta_i, \quad j = 1,3,5,\ldots,2p-1, \tag{13}$$

$$\begin{aligned}\gamma_j = & -[\phi_r \cos(\Phi_{\mathrm{sp}} + \Phi_{\mathrm{rp}}) + \theta_r \sin(\Phi_{\mathrm{sp}} + \Phi_{\mathrm{rp}})]\sin\alpha_i \\ & -[\phi_r \sin(\Phi_{\mathrm{sp}} + \Phi_{\mathrm{rp}}) - \theta_r \cos(\Phi_{\mathrm{sp}} + \Phi_{\mathrm{rp}})]\cos\alpha_i \\ & +\phi_i \sin(\Phi_{\mathrm{sp}} + \Phi_{\mathrm{rp}}) - \theta_i \cos(\Phi_{\mathrm{sp}} + \Phi_{\mathrm{rp}}), \quad j = 2,4,\ldots,2p.\end{aligned} \tag{14}$$

Lagrange's equations of motion are obtained following substitution of Eqs. (2)–(14) into the energy expressions in Eq. (1). In matrix form they are

$$\mathbf{M}\ddot{\mathbf{q}} + \Omega_c \mathbf{G}\dot{\mathbf{q}} + (\mathbf{K} - \Omega_c^2 \mathbf{C})\mathbf{q} = \Omega_c^2 \mathbf{c} + \mathbf{f}, \tag{15}$$

$$\mathbf{q} = (\mathbf{q}_s, \mathbf{q}_r, \mathbf{q}_c, \mathbf{q}_1, \ldots, \mathbf{q}_p),$$

$$\mathbf{q}_b = (\phi_b, \theta_b, \beta_b, x_b, y_b, z_b), \quad b = s,r,c,1,\ldots,p. \tag{16}$$

The diagonal inertia matrix $\mathbf{M}$ is

$$\mathbf{M} = \mathrm{diag}(\mathbf{M}_s, \mathbf{M}_r, \mathbf{M}_c, \mathbf{M}_1, \ldots, \mathbf{M}_i, \ldots, \mathbf{M}_p), \tag{17}$$

where an individual block is $\mathbf{M}_b = \mathrm{diag}(J_b^x, J_b^x, J_b^z, m_b, m_b, m_b)$. Only certain blocks of the stiffness matrix $\mathbf{K}$ are populated due to the geometric configuration of planetary gears. The $6N \times 6N$ matrix has the form

$$\mathbf{K} = \begin{bmatrix} \mathbf{K}_s & \mathbf{0} & \mathbf{0} & \mathbf{K}_{s,1} & \mathbf{K}_{s,2} & \ldots & \mathbf{K}_{s,p} \\ & \mathbf{K}_r & \mathbf{0} & \mathbf{K}_{r,1} & \mathbf{K}_{r,2} & \ldots & \mathbf{K}_{r,p} \\ & & \mathbf{K}_c & \mathbf{K}_{c,1} & \mathbf{K}_{c,2} & \ldots & \mathbf{K}_{c,p} \\ & & & \mathbf{K}_1 & \mathbf{0} & \ldots & \mathbf{0} \\ & & & & \mathbf{K}_2 & \ldots & \mathbf{0} \\ & \text{Symmetric} & & & & \ddots & \vdots \\ & & & & & & \mathbf{K}_p \end{bmatrix}_{n\times n}, \tag{18}$$

where the total number of degrees of freedom is $n = 6N$. The 6×6 sub-matrices $\mathbf{K}_h$, and $\mathbf{K}_{h,i}$, $h = s,r,c$, are expanded in the following section. The individual elements of these sub-matrices and of $\mathbf{K}_i$ are given in Appendix A. Spinning of the system generates the block diagonal gyroscopic matrix

$$\mathbf{G} = \mathrm{diag}(\mathbf{G}_s, \mathbf{G}_r, \mathbf{G}_c, \mathbf{G}_1, \ldots, \mathbf{G}_i, \ldots, \mathbf{G}_p), \tag{19}$$

$$\mathbf{G}_b = \begin{bmatrix} 0 & -R_b(2J_b^x - J_b^z) & 0 & 0 & 0 & 0 \\ R_b(2J_b^x - J_b^z) & 0 & 0 & 0 & 0 & 0 \\ 0 & 0 & 0 & 0 & 0 & 0 \\ 0 & 0 & 0 & 0 & -2m_b & 0 \\ 0 & 0 & 0 & 2m_b & 0 & 0 \\ 0 & 0 & 0 & 0 & 0 & 0 \end{bmatrix}, \tag{20}$$

where the gear ratios R_b relate the rotation speeds by $\Omega_b = R_b \Omega_c$ (recall $b = s,r,c,1,\ldots,p$). The centripetal stiffness matrix is

$$\mathbf{C} = \mathrm{diag}(\mathbf{C}_s, \mathbf{C}_r, \mathbf{C}_c, \mathbf{C}_1, \ldots, \mathbf{C}_i, \ldots, \mathbf{C}_p), \tag{21}$$

$$\mathbf{C}_b = \mathrm{diag}[J_b^x R_b^2, J_b^x R_b^2, 0, m_b, m_b, 0], \quad b = s,r,c,1,\ldots,p. \tag{22}$$

Carrier rotation induces constant planet centripetal accelerations evident in the $\Omega_c^2\mathbf{c}$ term of Eq. (15) where

$$\mathbf{c} = [\mathbf{0}, \mathbf{0}, \mathbf{0}, \mathbf{c}_1, \ldots, \mathbf{c}_i, \ldots, \mathbf{c}_p], \tag{23}$$

$$\mathbf{c}_i = m_p[0, 0, 0, -(r_s + r_p)\tan\Phi_{\mathrm{sp}}, r_s + r_p, 0]. \tag{24}$$

If one considers motion $\mathbf{y} = \mathbf{q} - \mathbf{q}_e$ about the steady configuration $\mathbf{q}_e$ defined by $(\mathbf{K} - \Omega_c^2\mathbf{C})\mathbf{q}_e = \Omega_c^2\mathbf{c} + \mathbf{f}$, where $\mathbf{f}$ is the constant external loading vector, the governing equation is

$$\mathbf{M}\ddot{\mathbf{y}} + \Omega_c\mathbf{G}\dot{\mathbf{y}} + (\mathbf{K} - \Omega_c^2\mathbf{C})\mathbf{y} = \mathbf{f}_d(t), \tag{25}$$

where $\mathbf{f}_d(t)$ is the zero-mean, dynamic external loading vector.

3. Modal analysis

3.1. Eigenvalue problem

The high-speed effects that arise from the constant kinematic rotation fall outside the scope of this study, so $\Omega_c = 0$ is specified. The eigenvalue problem is

$$(\mathbf{K} - \lambda\mathbf{M})\mathbf{q} = 0 \tag{26}$$

with natural frequencies $\sqrt{\lambda}$. The vibration modes are divided into 6×1 sub-vectors as

$$\mathbf{q} = (\mathbf{v}_s, \mathbf{v}_r, \mathbf{v}_c, \mathbf{v}_1, \ldots, \mathbf{v}_p). \tag{27}$$

The system is tuned, that is, all sun–planet and ring–planet mesh stiffnesses, and their centers of stiffnesses, are identical among all planets; the planet bearing stiffnesses, the axial locations of the planet bearings, and the planet inertias are the same for all planets. Regardless of planet spacing, the stiffness and inertia sub-matrices satisfy

$$\begin{aligned}\mathbf{K}_h = {} & \boldsymbol{\Upsilon}_h \sum_{i=1}^{p} \sin\alpha_i + \mathbf{R}\boldsymbol{\Upsilon}_h\mathbf{R}^{\mathrm{T}} \sum_{i=1}^{p} \cos\alpha_i + \boldsymbol{\Theta}_h \sum_{i=1}^{p} \sin^2\alpha_i \\ & + \mathbf{R}\boldsymbol{\Theta}_h\mathbf{R}^{\mathrm{T}} \sum_{i=1}^{p} \cos^2\alpha_i + \boldsymbol{\Xi}_h \sum_{i=1}^{p} \sin\alpha_i\cos\alpha_i + \boldsymbol{\Psi}_h, \quad h = s, r, c,\end{aligned} \tag{28}$$

$$\mathbf{R} = \begin{bmatrix} 0 & 1 & 0 & 0 & 0 & 0 \\ -1 & 0 & 0 & 0 & 0 & 0 \\ 0 & 0 & 1 & 0 & 0 & 0 \\ 0 & 0 & 0 & 0 & 1 & 0 \\ 0 & 0 & 0 & -1 & 0 & 0 \\ 0 & 0 & 0 & 0 & 0 & 1 \end{bmatrix}, \tag{29}$$

$$\mathbf{K}_i = \mathbf{K}_j, \quad \mathbf{M}_i = \mathbf{M}_j, \quad i, j = 1, 2, \ldots, p, \tag{30}$$

$$\mathbf{K}_{h,i} = \boldsymbol{\Lambda}_h \sin\alpha_i + \mathbf{R}\boldsymbol{\Lambda}_h \cos\alpha_i + \boldsymbol{\Gamma}_h. \tag{31}$$

Individual elements of $\boldsymbol{\Upsilon}_h$, $\boldsymbol{\Theta}_h$, $\boldsymbol{\Xi}_h$, $\boldsymbol{\Psi}_h$, $\boldsymbol{\Lambda}_h$, $\boldsymbol{\Gamma}_h$, and $\mathbf{K}_i$ are given in Appendix A.

3.2. Computational observation of vibration modes

Eigensolutions of a sample system (Table 1) with four and five equally spaced planets are evaluated numerically to expose the modal properties. Some natural frequencies and their corresponding mode types are given in Table 2. The vibration modes exhibit distinctive characteristics. There are three types of vibration modes. Figs. 3–6 show two examples of each of the three types of vibration modes for the example system with four planets. Regardless of the system parameters the modal deflections of certain gears are zero, or there is a

Table 1
Parameters of the planetary gear system.

Parameter	Sun	Mesh	Planet	Mesh	Ring	Carrier
Operating pressure angle, Φ (deg)		21.3		21.3		
Base helix angle, ψ (deg)		−28.5		28.5		
Translational mesh stiffness, k (N/m)		6.19×10^9		22.3×10^9		
Tilting mesh stiffness, κ (N m)		643×10^3		2.31×10^6		
Center of stiffness, c (mm)		0		0		
Base radius, r (mm)	24		16		56	
Center of mass, e (mm)	0		0		0	0
Bearing distance at point A, L^A (mm)	−20		−20		−20	−20
Bearing distance at point B, L^B (mm)	20		20		20	20
Radial bearing stiffnesses, k^A, k^B (N/m)	0.5×10^9		0.5×10^9		0.5×10^9	0.5×10^9
Axial bearing stiffnesses, k^{Az}, k^{Bz} (N/m)	0.5×10^9		0.5×10^9		0.5×10^9	0.5×10^9
Tilting bearing stiffnesses, κ^A, κ^B (N m)	50×10^6		5×10^6		50×10^6	50×10^6
Rotational bearing stiffnesses, κ^{Az}, κ^{Bz}(N m)	0		0		90×10^9	90×10^9
Mass, m (kg)	0.3		0.2		100×10^{-6}	0.5
Tilting inertia, J^x (kg m^2)	5×10^{-3}		50×10^{-6}		10×10^{-6}	4×10^{-3}
Rotational inertia, J^z (kg m^2)	10×10^{-3}		100×10^{-6}		20×10^{-6}	8×10^{-3}

Table 2
Lowest 10 natural frequencies (Hz) and mode types of the planetary gear system defined in Table 1 with four and five planets.

Four planets		Five planets	
Natural frequency (Hz)	Mode type	Natural frequency (Hz)	Mode type
953	R–A	1011	R–A
3120	T–T	3068	T–T
3120	T–T	3068	T–T
3251	R–A	3114	R–A
3743	R–A	3670	R–A
5426	T–T	5184	T–T
5426	T–T	5184	T–T
8177	P	8177	P
8537	T–T	8177	P
8537	T–T	8506	R–A

R–A: rotational–axial mode, T–T: translational–tilting mode, P: planet mode.

relation between certain degrees of freedom such that not all modal deflections are independent. Based on these features, all vibration modes are categorized as rotational–axial, translational–tilting, and planet modes. These three types bear some similarities to those described by Lin and Parker [5], but they have important differences.

3.2.1. Observed rotational–axial modes

There are 12 rotational–axial modes for systems with more than two planets. The natural frequency multiplicity is one. From the computed eigenvectors (in Fig. 3, for example) the central members rotate and translate axially, but they do not tilt or translate in-plane. The modal deflection of any central member is of the form

$$\mathbf{v}_h = (0, 0, \beta_h, 0, 0, z_h). \tag{32}$$

The planets move in all degrees of freedom, and their modal deflections are identical to one another as given by

$$\mathbf{v}_1 = \mathbf{v}_2 = \cdots = \mathbf{v}_p. \tag{33}$$

3.2.2. Observed translational–tilting modes

There are 12 pairs of translational–tilting modes with natural frequency multiplicity of two for systems with three or more planets. In both modes of a translational–tilting mode pair the central members only translate in-plane and tilt but do not rotate or translate axially. Figs. 4 and 5 show two examples of translational–tilting mode pairs. The modal deflections of any central member for a pair of vibration modes have the form

$$\mathbf{v}_h = (\phi_h, \theta_h, 0, x_h, y_h, 0), \quad \mathbf{w}_h = (\theta_h, -\phi_h, 0, y_h, -x_h, 0) \rightarrow \mathbf{w}_h = \mathbf{R}\mathbf{v}_h, \quad h = s, r, c. \tag{34}$$

The planets move in all six degrees of freedom. Their motions are such that the modal deflections of any planet can be found from the modal deflections of the arbitrarily selected first planet using

$$\begin{pmatrix} \mathbf{v}_i \\ \mathbf{w}_i \end{pmatrix} = \begin{bmatrix} \cos\alpha_i\mathbf{I} & \sin\alpha_i\mathbf{I} \\ -\sin\alpha_i\mathbf{I} & \cos\alpha_i\mathbf{I} \end{bmatrix} \begin{pmatrix} \mathbf{v}_1 \\ \mathbf{w}_1 \end{pmatrix}, \quad i = 2, \ldots, p, \tag{35}$$

where $\mathbf{I}$ is the 6×6 identity matrix.

3.2.3. Observed planet modes

In two sample planet modes shown in Fig. 6 all central members are stationary. This is given by

$$\mathbf{v}_h = \mathbf{0}, \quad h = s, r, c. \tag{36}$$

The planets move in all six degrees of freedom, and their motions are related to that of the arbitrarily selected first planet, as given by

$$\mathbf{v}_i = w_i\mathbf{v}_1, \quad i = 2, \ldots, p, \tag{37}$$

where the w_i are constants. Planet modes are observed only when there are four or more planets ($p \geqslant 4$). The natural frequency multiplicity is $p - 3$.

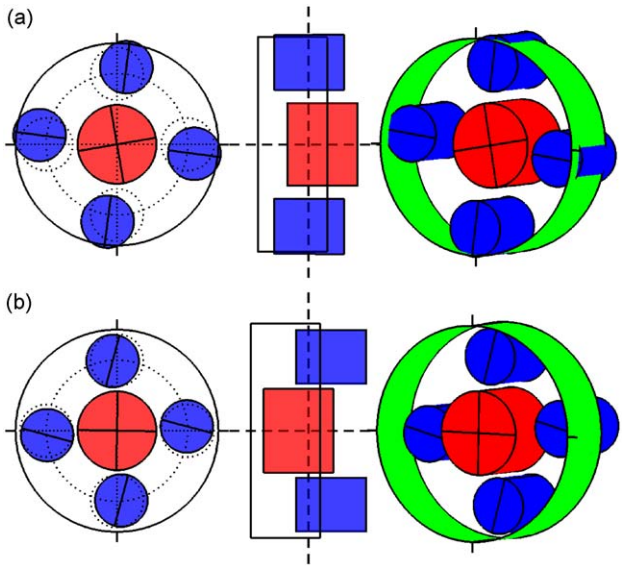

Fig. 3. Two rotational–axial modes of the planetary gear system defined in Table 1 with four equally spaced planets. Angular and translational displacements are scaled independently to emphasize behavior. (a) 953 Hz. (b) 3251 Hz.

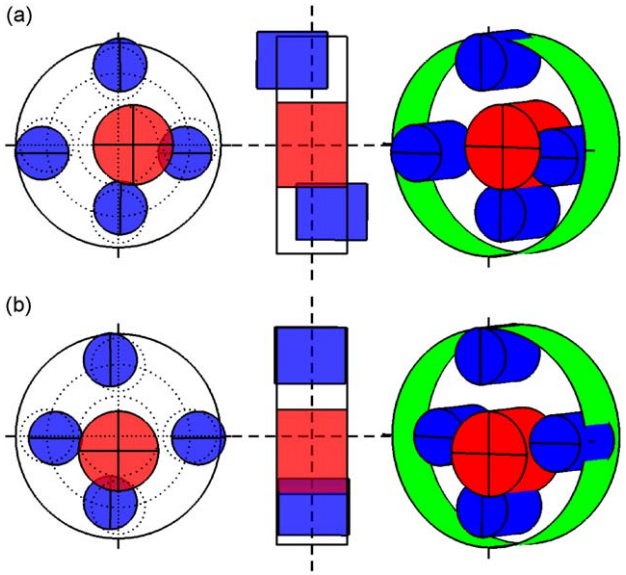

Fig. 4. A pair of degenerate translational–tilting modes (10 591 Hz) of the planetary gear system defined in Table 1 with four equally spaced planets. Angular and translational displacements are scaled independently to emphasize behavior.

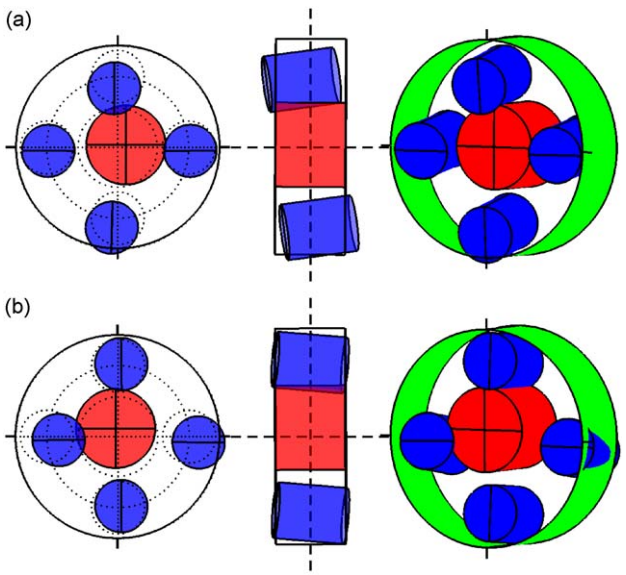

Fig. 5. A pair of degenerate translational–tilting modes (25 696 Hz) of the planetary gear system defined in Table 1 with four equally spaced planets. Angular and translational displacements are scaled independently to emphasize behavior.

3.3. Analytical characterization of vibration modes

The observed properties of the different types of vibration modes will be proved for general systems with three or more planets. The proof consists of constructing a candidate vibration mode (for each mode type) based on the observed characteristics and substituting it into the eigenvalue problem Eq. (26). Showing that the eigenvalue problem is satisfied ensures that the proposed vibration mode is truly a system vibration mode.

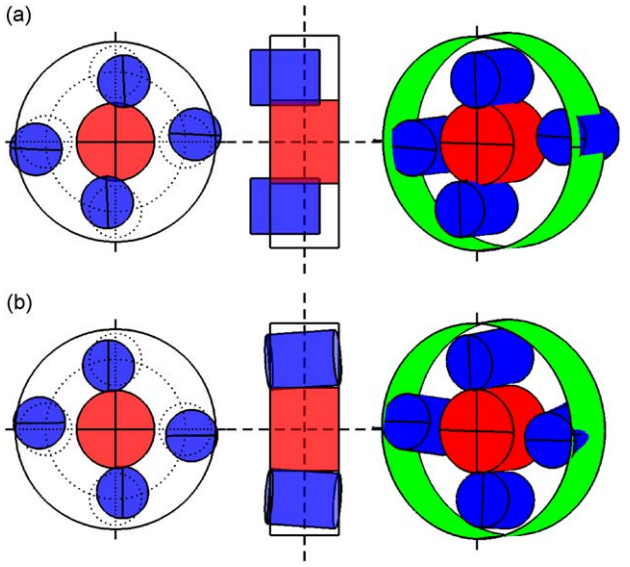

Fig. 6. Two planet modes of the planetary gear system defined in Table 1 with four equally spaced planets. Angular and translational displacements are scaled independently to emphasize behavior. (a) 8177 Hz. (b) 80 538 Hz.

The critical point for all three mode types is that some elements of the candidate vibration mode are linearly dependent on others. A candidate vibration mode is partitioned as

$$\mathbf{q} = (\mathbf{u}, \mathbf{q}^*), \quad \mathbf{q}^* = \mathbf{Y}\mathbf{u}, \tag{38}$$

where the vector $\mathbf{u}$ contains elements regarded as independent, and the vector $\mathbf{q}^*$ is the vector of dependent elements calculated from $\mathbf{u}$. How the modal deflections are partitioned between $\mathbf{u}$ and $\mathbf{q}^*$ as well as the matrix $\mathbf{Y}$ differ for each of the three mode types, but all three types can be expressed in this general form with known $\mathbf{Y}$. The three specific cases are discussed subsequently.

Substitution of the candidate vibration mode from Eq. (38) into the eigenvalue problem Eq. (26) results in

$$\begin{bmatrix} \mathbf{A} & \mathbf{B}^{\mathrm{T}} \\ \mathbf{B} & \mathbf{E} \end{bmatrix} \begin{pmatrix} \mathbf{u} \\ \mathbf{q}^* \end{pmatrix} = \lambda \begin{bmatrix} \mathbf{M}_u & \mathbf{0} \\ \mathbf{0} & \mathbf{M}_l \end{bmatrix} \begin{pmatrix} \mathbf{u} \\ \mathbf{q}^* \end{pmatrix}, \tag{39}$$

where $\mathbf{A}$, $\mathbf{B}$, and $\mathbf{E}$ are partitioned matrices of $\mathbf{K}$; $\mathbf{M}_u$ and $\mathbf{M}_l$ are partitioned matrices of the diagonal $\mathbf{M}$. The upper row yields $\mathbf{A}\mathbf{u} + \mathbf{B}^{\mathrm{T}}\mathbf{q}^* = \lambda\mathbf{M}_u\mathbf{u}$. Substitution of $\mathbf{q}^* = \mathbf{Y}\mathbf{u}$ expresses the upper row in the form of a reduced eigenvalue problem

$$(\mathbf{A} + \mathbf{B}^{\mathrm{T}}\mathbf{Y})\mathbf{u} = \lambda\mathbf{M}_u\mathbf{u}. \tag{40}$$

This equation contains all the necessary information to find the natural frequencies and vibration modes of the type of vibration mode under consideration. The remaining elements $\mathbf{q}^*$ of $\mathbf{q}$ are found from Eq. (38). *For such a mode to indeed be a system mode, however, the lower row of Eq.* (39) *must hold, which is given by*

$$\mathbf{B}\mathbf{u} + \mathbf{E}\mathbf{q}^* = \lambda\mathbf{M}_l\mathbf{q}^*. \tag{41}$$

This equation is crucial for the rest of this paper.

In what follows, we prove that Eq. (41) holds for appropriately selected candidate vibration modes of the form Eq. (38) constructed for each of the three mode types. In each case, $\mathbf{u}$ is calculated by the reduced eigenvalue problem in Eq. (40). In this process, the algebraic properties of the stiffness and inertia matrices are pivotal. Furthermore, we show that this process yields *all* of the system modes, that is, *every* mode is either a rotational–axial, translational–tilting, or planet mode.

Several elements of $\mathbf{q}^*$ are zero for each mode type. The non-zero elements are collected in $\mathbf{q}_N^*$. To simplify the subsequent algebra Eq. (41) is partitioned into two parts associated with the zero and non-zero elements of

$\mathbf{q}^*$ as

$$\begin{bmatrix} \mathbf{B}_0 \\ \mathbf{B}_N \end{bmatrix} \mathbf{u} + \left[\begin{array}{c|c} \mathrm{D}_0 & \mathrm{E}_0 \\ \hline \mathrm{D}_N & \mathrm{E}_N \end{array}\right] \begin{pmatrix} \mathbf{0} \\ \mathbf{q}_N^* \end{pmatrix} = \begin{pmatrix} \mathbf{0} \\ \lambda \mathbf{M}_N \mathbf{q}_N^* \end{pmatrix}, \tag{42}$$

where the subscripts 0 and N denote the partitioning, and Eq. (42) reflects $\mathbf{M}_l$ being diagonal. The upper and lower rows of Eq. (42) are

$$\mathbf{B}_0 \mathbf{u} + \mathbf{E}_0 \mathbf{q}_N^* = \mathbf{0}, \tag{43}$$

$$\mathbf{B}_N \mathbf{u} + \mathbf{E}_N \mathbf{q}_N^* = \lambda \mathbf{M}_N \mathbf{q}_N^*. \tag{44}$$

The construction of matrices $\mathbf{Y}$, $\mathbf{B}_0$, $\mathbf{B}_N$, $\mathbf{E}_0$, $\mathbf{E}_N$, $\mathbf{A}$, $\mathbf{M}_N$, and $\mathbf{M}_u$ are dictated by the partitioning of each candidate mode type by Eq. (38).

With the stipulations that the planets are equally spaced and the system is tuned, the following developments do not depend on, and are therefore valid for arbitrary values of, system parameters such as gear radii, pressure and helix angles, locations and stiffnesses of the bearings, mesh stiffnesses, and so on.

3.3.1. Rotational–axial modes

The decomposition of the candidate rotational–axial mode according to Eqs. (32), (33), and (38) is

$$\mathbf{u} = (\tilde{\mathbf{v}}_s, \tilde{\mathbf{v}}_r, \tilde{\mathbf{v}}_c, \mathbf{v}_1), \quad \mathbf{q}^* = (\mathbf{0}, \mathbf{0}, \mathbf{0}, \underbrace{\mathbf{v}_1, \ldots, \mathbf{v}_1}_{p-1}), \tag{45}$$

where the zero vector has dimension 4×1. The tilde accent is used here and for the other two mode types to represent sub-vectors containing only the independent elements $\mathbf{u}$ of the candidate mode $\mathbf{q}$ in Eq. (38). The specific elements in the quantities with a tilde accent will differ based on the mode type in question. The tilting and translational motions of the central members in a candidate rotational–axial mode are zero as indicated in Eq. (32), so the sun, ring, and carrier modal deflection sub-vectors are

$$\tilde{\mathbf{v}}_s = (\beta_s, z_s), \quad \tilde{\mathbf{v}}_r = (\beta_r, z_r), \quad \tilde{\mathbf{v}}_c = (\beta_c, z_c). \tag{46}$$

The modal deflections of each planet are identical as given by Eq. (33). The modal deflection of the arbitrarily selected first planet $\mathbf{v}_1$ is chosen to be the independent one hence the appearance of $\mathbf{v}_1$ in Eq. (45). The dependent elements contained in $\mathbf{q}^*$ are all calculable from the vector of independent elements $\mathbf{u}$ using Eq. (38) and

$$\mathbf{Y} = \begin{bmatrix} \mathbf{0}_{12\times 6} & \mathbf{0}_{12\times 6} \\ \mathbf{0}_{6\times 6} & \mathbf{I}_{6\times 6} \\ \vdots & \vdots \\ \mathbf{0}_{6\times 6} & \mathbf{I}_{6\times 6} \end{bmatrix} \tag{47}$$

with dimension $12 + 6(p-1) \times 12$.

One can readily partition Eq. (26) to obtain Eq. (39), and the reduced eigenvectors $\mathbf{u}$ are found from Eq. (40). To confirm that Eq. (45) is indeed a mode, each of Eqs. (43) and (44) must be satisfied for $\mathbf{u}$ and $\mathbf{q}^*$.

The matrices $\mathbf{B}_0$ and $\mathbf{E}_0$ in Eq. (43) are dictated by the partitioning given in Eq. (45) to be

$$\mathbf{B}_0 = \begin{bmatrix} \hat{\mathbf{K}}_s & \mathbf{0} & \mathbf{0} & \hat{\mathbf{K}}_{s,1} \\ \mathbf{0} & \hat{\mathbf{K}}_r & \mathbf{0} & \hat{\mathbf{K}}_{r,1} \\ \mathbf{0} & \mathbf{0} & \hat{\mathbf{K}}_c & \hat{\mathbf{K}}_{c,1} \end{bmatrix}, \quad \mathbf{E}_0 = \begin{bmatrix} \hat{\mathbf{K}}_{s,2} & \ldots & \hat{\mathbf{K}}_{s,p} \\ \hat{\mathbf{K}}_{r,2} & \ldots & \hat{\mathbf{K}}_{r,p} \\ \hat{\mathbf{K}}_{c,2} & \ldots & \hat{\mathbf{K}}_{c,p} \end{bmatrix}. \tag{48}$$

The sub-matrices $\hat{\mathbf{K}}_h$, $h = s, r, c$, are constructed from the 1st, 2nd, 4th, and 5th rows and 3rd and 6th columns of the corresponding matrices $\mathbf{K}_h$ in Eq. (18). The sub-matrices $\hat{\mathbf{K}}_{h,i}$, $i = 1, \ldots, p$, are constructed from the 1st, 2nd, 4th, and 5th rows and all columns of the corresponding matrices $\mathbf{K}_{h,i}$ in Eq. (18). $\mathbf{B}_0$ has dimension 12×12 and $\mathbf{E}_0$ has dimension $12 \times 6(p-1)$.

Substitution of matrices $\mathbf{B}_0$ and $\mathbf{E}_0$ from Eq. (48) into Eq. (43) yields

$$\hat{\mathbf{K}}_h\tilde{\mathbf{v}}_h+\sum_{i=1}^{p}\hat{\mathbf{K}}_{h,i}\mathbf{v}_1=\mathbf{0}. \tag{49}$$

From Eq. (28), the sub-matrices $\hat{\mathbf{K}}_h$ satisfy

$$\hat{\mathbf{K}}_h=\hat{\boldsymbol{\Upsilon}}_h\sum_{i=1}^{p}\sin\alpha_i+\bar{\mathbf{R}}\hat{\boldsymbol{\Upsilon}}_h\hat{\mathbf{R}}^{\mathrm{T}}\sum_{i=1}^{p}\cos\alpha_i, \tag{50}$$

because $\hat{\boldsymbol{\Theta}}_h=\hat{\boldsymbol{\Xi}}_h=\hat{\boldsymbol{\Psi}}_h=\mathbf{0}$ by Eqs. (88)–(90), (94)–(96), (100)–(102). The hat accent on $\hat{\mathbf{R}}$ indicates the 3rd and 6th rows and 3rd and 6th columns of $\mathbf{R}$. The bar accent on $\bar{\mathbf{R}}$ indicates the 1st, 2nd, 4th, and 5th rows and the 1st, 2nd, 4th, and 5th columns of $\mathbf{R}$. From Ref. [23]

$$\sum_{i=1}^{p}\sin i\alpha=\frac{\sin\frac{p+1}{2}\alpha\sin\frac{p\alpha}{2}}{\sin\frac{\alpha}{2}}=0,\ \sum_{i=0}^{p}\cos i\alpha=\frac{\cos\frac{p+1}{2}\alpha\sin\frac{p\alpha}{2}}{\sin\frac{\alpha}{2}}+1=0, \tag{51}$$

where the second equalities are from equal planet spacing $\alpha=2\pi/p$. The sub-matrices $\hat{\mathbf{K}}_h$ in Eq. (49) vanish as a result of Eqs. (50) and (51). For vanishing $\hat{\mathbf{K}}_h$ Eq. (49) becomes, after use of Eq. (31) and $\hat{\boldsymbol{\Gamma}}_h=\mathbf{0}$ (by Eqs. (92), (98), and (104))

$$\sum_{i=1}^{p}\hat{\mathbf{K}}_{h,i}\mathbf{v}_1=\hat{\boldsymbol{\Lambda}}_h\mathbf{v}_1\sum_{i=1}^{p}\sin\alpha_i+\bar{\mathbf{R}}\hat{\boldsymbol{\Lambda}}_h\mathbf{v}_1\sum_{i=1}^{p}\cos\alpha_i=\mathbf{0}, \tag{52}$$

where the second equality results from Eq. (51). This confirms that Eq. (43) is satisfied for the candidate rotational–axial vibration mode defined in Eq. (45).

We now examine whether Eq. (44) is satisfied. The matrices $\mathbf{B}_N$, $\mathbf{E}_N$, and $\mathbf{M}_N$ are

$$\mathbf{B}_N=\begin{bmatrix}\bar{\mathbf{K}}_{s,2}^{\mathrm{T}} & \bar{\mathbf{K}}_{r,2}^{\mathrm{T}} & \bar{\mathbf{K}}_{c,2}^{\mathrm{T}} & \mathbf{0}\\ \vdots & \vdots & \vdots & \vdots\\ \bar{\mathbf{K}}_{s,p}^{\mathrm{T}} & \bar{\mathbf{K}}_{r,p}^{\mathrm{T}} & \bar{\mathbf{K}}_{c,p}^{\mathrm{T}} & \mathbf{0}\end{bmatrix},\quad \mathbf{E}_N=\mathrm{diag}(\mathbf{K}_2,\ldots,\mathbf{K}_p),\quad \mathbf{M}_N=\mathrm{diag}(\mathbf{M}_2,\ldots,\mathbf{M}_p). \tag{53}$$

The sub-matrices $\bar{\mathbf{K}}_{h,i}$ are constructed from all columns and the 3rd and 6th rows of $\mathbf{K}_{h,i}$ in Eq. (18), so using Eq. (31) and $\bar{\boldsymbol{\Lambda}}_h=\mathbf{0}$ (by Eqs. (91), (97), (103)) Eq. (31) becomes

$$\bar{\mathbf{K}}_{h,i}=\bar{\boldsymbol{\Gamma}}_h. \tag{54}$$

The zero matrices are 6×6. The matrices $\mathbf{B}_N$, $\mathbf{E}_N$, and $\mathbf{M}_N$ have dimensions $6(p-1)\times 12$, $6(p-1)\times 6(p-1)$, and $6(p-1)\times 6(p-1)$, respectively. Substitution of Eq. (53) into Eq. (44) yields $p-1$ matrix equations $\sum_{h=s,r,c}\bar{\boldsymbol{\Gamma}}_h^{\mathrm{T}}\tilde{\mathbf{v}}_h+\mathbf{K}_i\mathbf{v}_1=\lambda\mathbf{M}_i\mathbf{v}_1$, $i=2,\ldots,p$. Substitution of Eq. (30) gives

$$\sum_{h=s,r,c}\bar{\boldsymbol{\Gamma}}_h^{\mathrm{T}}\tilde{\mathbf{v}}_h+\mathbf{K}_1\mathbf{v}_1=\lambda\mathbf{M}_1\mathbf{v}_1. \tag{55}$$

We now show that this equality is satisfied for $\tilde{\mathbf{v}}_h$ and $\mathbf{v}_1$ calculated from the reduced eigenvalue problem Eq. (40). The matrices $\mathbf{A}$ and $\mathbf{M}_u$ in Eq. (40) are

$$\mathbf{A}=\begin{bmatrix}\acute{\mathbf{K}}_s & \mathbf{0} & \mathbf{0} & \bar{\mathbf{K}}_{s,1}\\ \mathbf{0} & \acute{\mathbf{K}}_r & \mathbf{0} & \bar{\mathbf{K}}_{r,1}\\ \mathbf{0} & \mathbf{0} & \acute{\mathbf{K}}_c & \bar{\mathbf{K}}_{c,1}\\ \bar{\mathbf{K}}_{s,1}^{\mathrm{T}} & \bar{\mathbf{K}}_{r,1}^{\mathrm{T}} & \bar{\mathbf{K}}_{c,1}^{\mathrm{T}} & \mathbf{K}_1\end{bmatrix},\quad \mathbf{M}_u=\mathrm{diag}(\acute{\mathbf{M}}_s,\acute{\mathbf{M}}_r,\acute{\mathbf{M}}_c,\mathbf{M}_1), \tag{56}$$

where $\acute{\mathbf{M}}_h$ and $\acute{\mathbf{K}}_h$ are constructed from the 3rd and 6th rows and the 3rd and 6th columns of the corresponding matrices in Eqs. (17) and (18). The matrices $\mathbf{A}$ and $\mathbf{M}_u$ have dimension 12×12. Upon substitution of $\mathbf{A}$, $\mathbf{M}_u$, $\mathbf{B}_0$, $\mathbf{B}_N$, and $\mathbf{Y}$ from Eqs. (56), (48), (53), (47), and (54) into Eq. (40), the reduced

eigenvalue problem for rotational–axial modes is

$$\begin{bmatrix} \acute{\mathbf{K}}_s & 0 & 0 & p\bar{\mathbf{\Gamma}}_s \\ 0 & \acute{\mathbf{K}}_r & 0 & p\bar{\mathbf{\Gamma}}_r \\ 0 & 0 & \acute{\mathbf{K}}_c & p\bar{\mathbf{\Gamma}}_c \\ p\bar{\mathbf{\Gamma}}_s^{\mathrm{T}} & p\bar{\mathbf{\Gamma}}_r^{\mathrm{T}} & p\bar{\mathbf{\Gamma}}_c^{\mathrm{T}} & p\mathbf{K}_1 \end{bmatrix} \begin{pmatrix} \tilde{\mathbf{v}}_s \\ \tilde{\mathbf{v}}_r \\ \tilde{\mathbf{v}}_c \\ \mathbf{v}_1 \end{pmatrix} = \lambda \begin{bmatrix} \acute{\mathbf{M}}_s & 0 & 0 & 0 \\ 0 & \acute{\mathbf{M}}_r & 0 & 0 \\ 0 & 0 & \acute{\mathbf{M}}_c & 0 \\ 0 & 0 & 0 & p\mathbf{M}_1 \end{bmatrix} \begin{pmatrix} \tilde{\mathbf{v}}_s \\ \tilde{\mathbf{v}}_r \\ \tilde{\mathbf{v}}_c \\ \mathbf{v}_1 \end{pmatrix}. \tag{57}$$

The last row of the reduced eigenvalue problem in Eq. (57) is the same equation as Eq. (55). Thus, $\mathbf{u}$ satisfying Eq. (40) ensures the satisfaction of Eq. (55), and so the satisfaction of Eq. (44).

We have shown that every rotational–axial mode $\mathbf{q}$ of the form Eqs. (38) and (45), defined by Eqs. (32) and (33) satisfies the full eigenvalue problem Eq. (26); each $\mathbf{u}$ is determined from the reduced eigenvalue problem Eq. (40). In the rotational–axial mode case, Eq. (40) is a 12×12 eigenvalue problem and the reduced eigenvector $\mathbf{u}$ has 12 elements. Therefore, there are 12 rotational–axial modes. Because each reduced eigenvector $\mathbf{u}$ produces only one rotational–axial mode, each rotational–axial mode has a distinct natural frequency.

3.3.2. Translational–tilting modes

The candidate pair of translational–tilting modes given by the relations Eqs. (34) and (35) satisfy the eigenvalue problem Eq. (26) with the same eigenvalue. This is expressed as

$$(\mathbf{K} - \lambda\mathbf{M})\mathbf{q}_1 = \mathbf{0}, \quad (\mathbf{K} - \lambda\mathbf{M})\mathbf{q}_2 = \mathbf{0}. \tag{58}$$

Any linear combination of $\mathbf{q}_1$ and $\mathbf{q}_2$ also satisfies the full eigenvalue problem with the same eigenvalue. To apply the formulation in Eqs. (40)–(44), we stack the two expressions in Eq. (58) into a single block-diagonal matrix eigenvalue problem of dimension $12(p+3)$ with eigenvector

$$\mathbf{q} = (\mathbf{q}_1, \mathbf{q}_2). \tag{59}$$

This eigenvalue problem is partitioned to give Eq. (39). To that end, decomposition of the candidate translational–tilting mode pair in Eq. (59) according to Eqs. (34), (35), and (38) gives

$$\mathbf{u} = (\tilde{\mathbf{v}}_s, \tilde{\mathbf{v}}_r, \tilde{\mathbf{v}}_c, \mathbf{v}_1, \mathbf{w}_1),$$

$$\mathbf{q}^* = (\mathbf{0}, \mathbf{0}, \mathbf{0}, \mathbf{w}_s, \mathbf{w}_r, \mathbf{w}_c, \mathbf{v}_2, \ldots, \mathbf{v}_p, \mathbf{w}_2, \ldots, \mathbf{w}_p), \tag{60}$$

where the zero vectors are 2×1. The matrix $\mathbf{Y}$ combines Eqs. (34) and (35) to relate $\mathbf{q}^*$ to $\mathbf{u}$ in Eq. (38), and it is given by

$$\mathbf{Y} = \begin{bmatrix} \mathbf{0}_{6\times4} & \mathbf{0}_{6\times4} & \mathbf{0}_{6\times4} & \mathbf{0}_{6\times6} & \mathbf{0}_{6\times6} \\ \bar{\mathbf{R}} & \mathbf{0}_{4\times4} & \mathbf{0}_{4\times4} & \mathbf{0}_{4\times6} & \mathbf{0}_{4\times6} \\ \mathbf{0}_{4\times4} & \bar{\mathbf{R}} & \mathbf{0}_{4\times4} & \mathbf{0}_{4\times6} & \mathbf{0}_{4\times6} \\ \mathbf{0}_{4\times4} & \mathbf{0}_{4\times4} & \bar{\mathbf{R}} & \mathbf{0}_{4\times6} & \mathbf{0}_{4\times6} \\ \mathbf{0}_{6\times6} & \mathbf{0}_{6\times6} & \mathbf{0}_{6\times6} & \mathbf{I}\cos\alpha_2 & \mathbf{I}\sin\alpha_2 \\ \vdots & \vdots & \vdots & \vdots & \vdots \\ \mathbf{0}_{6\times6} & \mathbf{0}_{6\times6} & \mathbf{0}_{6\times6} & \mathbf{I}\cos\alpha_p & \mathbf{I}\sin\alpha_p \\ \mathbf{0}_{6\times6} & \mathbf{0}_{6\times6} & \mathbf{0}_{6\times6} & -\mathbf{I}\sin\alpha_2 & \mathbf{I}\cos\alpha_2 \\ \vdots & \vdots & \vdots & \vdots & \vdots \\ \mathbf{0}_{6\times6} & \mathbf{0}_{6\times6} & \mathbf{0}_{6\times6} & -\mathbf{I}\sin\alpha_p & \mathbf{I}\cos\alpha_p \end{bmatrix}, \tag{61}$$

where the bar accent on $\bar{\mathbf{R}}$ indicates the 1st, 2nd, 4th, and 5th rows and the 1st, 2nd, 4th, and 5th columns of $\mathbf{R}$.

The sub-matrices $\mathbf{B}_0$ and $\mathbf{E}_0$ in Eq. (43) are

$$\mathbf{B}_0 = \begin{bmatrix} \hat{\mathbf{K}}_s & \mathbf{0} & \mathbf{0} & \hat{\mathbf{K}}_{s,1} & \hat{\mathbf{K}}_{s,1} \\ \mathbf{0} & \hat{\mathbf{K}}_r & \mathbf{0} & \hat{\mathbf{K}}_{r,1} & \hat{\mathbf{K}}_{r,1} \\ \mathbf{0} & \mathbf{0} & \hat{\mathbf{K}}_c & \hat{\mathbf{K}}_{c,1} & \hat{\mathbf{K}}_{c,1} \end{bmatrix}, \tag{62}$$

$$\mathbf{E}_0 = \begin{bmatrix} \hat{\mathbf{K}}_s & \mathbf{0} & \mathbf{0} & \hat{\mathbf{K}}_{s,2} & \dots & \hat{\mathbf{K}}_{s,p} & \hat{\mathbf{K}}_{s,2} & \dots & \hat{\mathbf{K}}_{s,p} \\ \mathbf{0} & \hat{\mathbf{K}}_r & \mathbf{0} & \hat{\mathbf{K}}_{r,2} & \dots & \hat{\mathbf{K}}_{r,p} & \hat{\mathbf{K}}_{r,2} & \dots & \hat{\mathbf{K}}_{r,p} \\ \mathbf{0} & \mathbf{0} & \hat{\mathbf{K}}_c & \hat{\mathbf{K}}_{c,2} & \dots & \hat{\mathbf{K}}_{c,p} & \hat{\mathbf{K}}_{c,2} & \dots & \hat{\mathbf{K}}_{c,p} \end{bmatrix}. \tag{63}$$

The sub-matrices $\hat{\mathbf{K}}_h$ are constructed from the 1st, 2nd, 4th, and 5th columns and the 3rd and 6th rows of the corresponding matrices in Eq. (18). The sub-matrices $\hat{\mathbf{K}}_{h,i}$ are constructed from all columns and the 3rd and 6th rows of the corresponding matrices in Eq. (18). $\mathbf{B}_0$ has dimension 6×24 and $\mathbf{E}_0$ has dimension $6 \times 12p$.

Substitution of $\mathbf{B}_0$ and $\mathbf{E}_0$ from Eqs. (62) and (63) into Eq. (43) yields

$$\hat{\mathbf{K}}_h \tilde{\mathbf{v}}_h + \sum_{i=1}^{p} \hat{\mathbf{K}}_{h,i} \mathbf{v}_i = \mathbf{0}, \quad \hat{\mathbf{K}}_h \tilde{\mathbf{w}}_h + \sum_{i=1}^{p} \hat{\mathbf{K}}_{h,i} \mathbf{w}_i = \mathbf{0}, \;\; h = s, r, c. \tag{64}$$

Considering the specified $\hat{\mathbf{K}}_h$ and Eq. (28), $\hat{\mathbf{\Theta}}_h = \hat{\mathbf{\Xi}}_h = \hat{\mathbf{\Psi}}_h = \mathbf{0}$ by Eqs. (88)–(90), (94)–(96), (100)–(102). Thus, using Eq. (51), the sub-matrices $\hat{\mathbf{K}}_h$ vanish for equally spaced planets. Use of Eq. (31) and $\hat{\mathbf{\Lambda}}_h = \mathbf{0}$ (by Eqs. (91), (97), and (103)) simplifies the off-diagonal sub-matrices to $\hat{\mathbf{K}}_{h,i} = \hat{\mathbf{\Gamma}}_h$. For vanishing $\hat{\mathbf{K}}_h$, substitution of Eq. (35) into Eq. (64) yields

$$\hat{\mathbf{\Gamma}}_h \sum_{i=1}^{p} \mathbf{v}_1 \cos\alpha_i + \mathbf{w}_1 \sin\alpha_i = \mathbf{0}, \quad \hat{\mathbf{\Gamma}}_h \sum_{i=1}^{p} \mathbf{w}_1 \cos\alpha_i - \mathbf{v}_1 \sin\alpha_i = \mathbf{0}, \;\; h = s, r, c. \tag{65}$$

These six matrix equations are satisfied in light of Eq. (51). This confirms that Eq. (43) is satisfied for the candidate mode given in Eq. (60), or equivalently, Eqs. (34) and (35).

The matrices $\mathbf{B}_N$, $\mathbf{E}_N$, and $\mathbf{M}_N$ in Eq. (44) are given by

$$\mathbf{B}_N = \begin{bmatrix} \mathbf{0}_{4\times4} & \mathbf{0}_{4\times4} & \mathbf{0}_{4\times4} & \mathbf{0}_{4\times6} & \bar{\mathbf{K}}_{s,1} \\ \mathbf{0}_{4\times4} & \mathbf{0}_{4\times4} & \mathbf{0}_{4\times4} & \mathbf{0}_{4\times6} & \bar{\mathbf{K}}_{r,1} \\ \mathbf{0}_{4\times4} & \mathbf{0}_{4\times4} & \mathbf{0}_{4\times4} & \mathbf{0}_{4\times6} & \bar{\mathbf{K}}_{c,1} \\ \bar{\mathbf{K}}_{s,2}^{\mathrm{T}} & \bar{\mathbf{K}}_{r,2}^{\mathrm{T}} & \bar{\mathbf{K}}_{c,2}^{\mathrm{T}} & \mathbf{0}_{6\times6} & \mathbf{0}_{6\times6} \\ \vdots & \vdots & \vdots & \vdots & \vdots \\ \bar{\mathbf{K}}_{s,p}^{\mathrm{T}} & \bar{\mathbf{K}}_{r,p}^{\mathrm{T}} & \bar{\mathbf{K}}_{c,p}^{\mathrm{T}} & \mathbf{0}_{6\times6} & \mathbf{0}_{6\times6} \\ \mathbf{0}_{6(p-1)\times4} & \mathbf{0}_{6(p-1)\times4} & \mathbf{0}_{6(p-1)\times4} & \mathbf{0}_{6(p-1)\times6} & \mathbf{0}_{6(p-1)\times6} \end{bmatrix}, \tag{66}$$

$$\mathbf{E}_N = \begin{bmatrix} \acute{\mathbf{K}}_s & \mathbf{0}_{4\times4} & \mathbf{0}_{4\times4} & \mathbf{0}_{4\times6} & \cdots & \mathbf{0}_{4\times6} & \bar{\mathbf{K}}_{s,2} & \cdots & \bar{\mathbf{K}}_{s,p} \\ \mathbf{0}_{4\times4} & \acute{\mathbf{K}}_r & \mathbf{0}_{4\times4} & \mathbf{0}_{4\times6} & \cdots & \mathbf{0}_{4\times6} & \bar{\mathbf{K}}_{r,2} & \cdots & \bar{\mathbf{K}}_{r,p} \\ \mathbf{0}_{4\times4} & \mathbf{0}_{4\times4} & \acute{\mathbf{K}}_c & \mathbf{0}_{4\times6} & \cdots & \mathbf{0}_{4\times6} & \bar{\mathbf{K}}_{c,2} & \cdots & \bar{\mathbf{K}}_{c,p} \\ \mathbf{0}_{6\times4} & \mathbf{0}_{6\times4} & \mathbf{0}_{6\times4} & \mathbf{K}_2 & \cdots & \mathbf{0}_{6\times6} & \mathbf{0}_{6\times6} & \cdots & \mathbf{0}_{6\times4} \\ \vdots & \vdots & \vdots & \vdots & \ddots & \vdots & \vdots & \ddots & \vdots \\ \mathbf{0}_{6\times4} & \mathbf{0}_{6\times4} & \mathbf{0}_{6\times4} & \mathbf{0}_{6\times6} & \cdots & \mathbf{K}_p & \mathbf{0}_{6\times6} & \cdots & \mathbf{0}_{6\times4} \\ \bar{\mathbf{K}}_{s,2}^{\mathrm{T}} & \bar{\mathbf{K}}_{r,2}^{\mathrm{T}} & \bar{\mathbf{K}}_{c,2}^{\mathrm{T}} & \mathbf{0}_{6\times6} & \cdots & \mathbf{0}_{6\times6} & \mathbf{K}_2 & \cdots & \mathbf{0}_{6\times6} \\ \vdots & \vdots & \vdots & \vdots & \ddots & \vdots & \vdots & \ddots & \vdots \\ \bar{\mathbf{K}}_{s,p}^{\mathrm{T}} & \bar{\mathbf{K}}_{r,p}^{\mathrm{T}} & \bar{\mathbf{K}}_{c,p}^{\mathrm{T}} & \mathbf{0}_{6\times6} & \cdots & \mathbf{0}_{6\times6} & \mathbf{0}_{6\times6} & \cdots & \mathbf{K}_p \end{bmatrix}, \tag{67}$$

$$\mathbf{M}_N = \mathrm{diag}(\acute{\mathbf{M}}_s, \acute{\mathbf{M}}_r, \acute{\mathbf{M}}_c, \mathbf{M}_2, \ldots, \mathbf{M}_p, \mathbf{M}_2, \ldots, \mathbf{M}_p). \tag{68}$$

The sub-matrices $\bar{\mathbf{K}}_{h,i}$ are constructed from all columns and the 1st, 2nd, 4th, and 5th rows of the corresponding matrices in Eq. (18). Use of Eq. (31) and $\bar{\mathbf{\Gamma}}_h = \mathbf{0}$ (by Eqs. (92), (98), and (104)) simplifies the off-diagonal sub-matrices to

$$\bar{\mathbf{K}}_{h,i} = \bar{\mathbf{\Lambda}}_h. \tag{69}$$

The sub-matrices $\acute{\mathbf{M}}_h$ and $\acute{\mathbf{K}}_h$ are constructed from the 1st, 2nd, 4th, and 5th rows and the 1st, 2nd, 4th, and 5th columns from the corresponding matrices in Eqs. (17) and (18). The planet stiffness and inertia sub-matrices $\mathbf{M}_i$ and $\mathbf{K}_i$ do not need partitioning; they are identical to the ones in Eqs. (17) and (18). $\mathbf{B}_N$ has dimension $12p \times 24$, and $\mathbf{E}_N$ and $\mathbf{M}_N$ have dimension $12p \times 12p$.

Substitution of Eqs. (66)–(68), and the candidate mode from Eq. (60) into Eq. (44) gives

$$\acute{\mathbf{K}}_h \tilde{\mathbf{w}}_h + \sum_{i=1}^{p} \bar{\mathbf{K}}_{h,i} \mathbf{w}_i = \lambda \acute{\mathbf{M}}_h \tilde{\mathbf{w}}_h, \quad h = s, r, c, \tag{70}$$

$$\sum_{h=s,r,c} \bar{\mathbf{K}}_{h,i}^{\mathrm{T}} \mathbf{v}_h + \mathbf{K}_i \mathbf{v}_i = \lambda \mathbf{M}_i \mathbf{v}_i, \quad i = 2, \ldots, p, \tag{71}$$

$$\sum_{h=s,r,c} \bar{\mathbf{K}}_{h,i}^{\mathrm{T}} \mathbf{w}_h + \mathbf{K}_i \mathbf{w}_i = \lambda \mathbf{M}_i \mathbf{w}_i, \quad i = 2, \ldots, p. \tag{72}$$

From Ref. [23]

$$\sum_{i=1}^{p} \sin^2 i\alpha = \frac{p}{2} - \frac{\cos(p+1)\alpha \sin p\alpha}{2 \sin \alpha} = \frac{p}{2}, \quad \sum_{i=1}^{p} \cos^2 i\alpha = \frac{p}{2} + \frac{\cos(p+1)\alpha \sin p\alpha}{2 \sin \alpha} = \frac{p}{2},$$

$$\sum_{i=1}^{p} \sin i\alpha \cos i\alpha = \frac{\sin(p+1)\alpha \sin p\alpha}{2 \sin \alpha} = 0, \tag{73}$$

where the second equalities result from equal planet spacing $\alpha = 2\pi/p$. Substitution of Eqs. (34), (35), and (73) into Eq. (70), premultiplication by $\bar{\mathbf{R}}^{\mathrm{T}}$, and use of $\bar{\mathbf{R}}^{\mathrm{T}} \acute{\mathbf{M}}_h \bar{\mathbf{R}} = \acute{\mathbf{M}}_h$, $\bar{\mathbf{R}}^{\mathrm{T}} \acute{\mathbf{K}}_h \bar{\mathbf{R}} = \acute{\mathbf{K}}_h$ gives

$$\acute{\mathbf{K}}_h \tilde{\mathbf{v}}_h + \frac{p}{2} \bar{\mathbf{R}} \bar{\mathbf{\Lambda}}_h \mathbf{v}_1 + \frac{p}{2} \bar{\mathbf{\Lambda}}_h \mathbf{w}_1 = \lambda \acute{\mathbf{M}}_h \tilde{\mathbf{v}}_h, \quad h = s, r, c. \tag{74}$$

Substitution of Eqs. (30), (34), and (35) into Eqs. (71) and (72), and summing the $p-1$ equations, gives (for $\alpha_1=0$ and $\bar{\mathbf{R}}^{\mathrm{T}}\bar{\mathbf{R}}=\mathbf{I}$)

$$\left(\sum_{h=s,r,c}\bar{\mathbf{\Lambda}}_h^{\mathrm{T}}\bar{\mathbf{R}}^{\mathrm{T}}\tilde{\mathbf{v}}_h+\mathbf{K}_1\mathbf{v}_1-\lambda\mathbf{M}_1\mathbf{v}_1\right)\sum_{i=2}^{p}\cos\alpha_i=\mathbf{0}, \tag{75}$$

$$\left(\sum_{h=s,r,c}\bar{\mathbf{\Lambda}}_h^{\mathrm{T}}\tilde{\mathbf{v}}_h+\mathbf{K}_1\mathbf{w}_1-\lambda\mathbf{M}_1\mathbf{w}_1\right)\sum_{i=2}^{p}\cos\alpha_i=\mathbf{0}. \tag{76}$$

We now show that Eqs. (74)–(76) are satisfied for $\tilde{\mathbf{v}}_h$, $\tilde{\mathbf{w}}_h$, $\mathbf{v}_i$, and $\mathbf{w}_i$ calculated from the reduced eigenvalue problem Eq. (40). $\mathbf{A}$ and $\mathbf{M}_u$ are given by

$$\mathbf{A}=\begin{bmatrix}\acute{\mathbf{K}}_s & \mathbf{0}_{4\times4} & \mathbf{0}_{4\times4} & \bar{\mathbf{K}}_{s,1} & \mathbf{0}_{4\times6}\\ \mathbf{0}_{4\times4} & \acute{\mathbf{K}}_r & \mathbf{0}_{4\times4} & \bar{\mathbf{K}}_{r,1} & \mathbf{0}_{4\times6}\\ \mathbf{0}_{4\times4} & \mathbf{0}_{4\times4} & \acute{\mathbf{K}}_c & \bar{\mathbf{K}}_{c,1} & \mathbf{0}_{4\times6}\\ \bar{\mathbf{K}}_{s,1}^{\mathrm{T}} & \bar{\mathbf{K}}_{r,1}^{\mathrm{T}} & \bar{\mathbf{K}}_{c,1}^{\mathrm{T}} & \mathbf{K}_1 & \mathbf{0}_{6\times6}\\ \mathbf{0}_{6\times4} & \mathbf{0}_{6\times4} & \mathbf{0}_{6\times4} & \mathbf{0}_{6\times6} & \mathbf{K}_1\end{bmatrix},\quad \mathbf{M}_u=\mathrm{diag}(\acute{\mathbf{M}}_s,\acute{\mathbf{M}}_r,\acute{\mathbf{M}}_c,\mathbf{M}_1). \tag{77}$$

Substitution of $\mathbf{A}$, $\mathbf{M}_u$, $\mathbf{B}_0$, $\mathbf{B}_N$, and $\mathbf{Y}$ from Eqs. (77), (62), (66), (61), and (69) into Eq. (40), and using algebra similar to that in Eqs. (74)–(76), gives the 24×24 reduced eigenvalue problem

$$\begin{bmatrix}\acute{\mathbf{K}}_s & \mathbf{0}_{4\times4} & \mathbf{0}_{4\times4} & \frac{p}{2}\bar{\mathbf{R}}\bar{\mathbf{\Lambda}}_s & \frac{p}{2}\bar{\mathbf{\Lambda}}_s\\ \mathbf{0}_{4\times4} & \acute{\mathbf{K}}_r & \mathbf{0}_{4\times4} & \frac{p}{2}\bar{\mathbf{R}}\bar{\mathbf{\Lambda}}_r & \frac{p}{2}\bar{\mathbf{\Lambda}}_r\\ \mathbf{0}_{4\times4} & \mathbf{0}_{4\times4} & \acute{\mathbf{K}}_c & \frac{p}{2}\bar{\mathbf{R}}\bar{\mathbf{\Lambda}}_c & \frac{p}{2}\bar{\mathbf{\Lambda}}_c\\ \frac{p}{2}\bar{\mathbf{\Lambda}}_s^{\mathrm{T}}\bar{\mathbf{R}}^{\mathrm{T}} & \frac{p}{2}\bar{\mathbf{\Lambda}}_r^{\mathrm{T}}\bar{\mathbf{R}}^{\mathrm{T}} & \frac{p}{2}\bar{\mathbf{\Lambda}}_c^{\mathrm{T}}\bar{\mathbf{R}}^{\mathrm{T}} & \frac{p}{2}\mathbf{K}_1 & \mathbf{0}_{6\times6}\\ \frac{p}{2}\bar{\mathbf{\Lambda}}_s^{\mathrm{T}} & \frac{p}{2}\bar{\mathbf{\Lambda}}_r^{\mathrm{T}} & \frac{p}{2}\bar{\mathbf{\Lambda}}_c^{\mathrm{T}} & \mathbf{0}_{6\times6} & \frac{p}{2}\mathbf{K}_1\end{bmatrix}\begin{pmatrix}\tilde{\mathbf{v}}_s\\ \tilde{\mathbf{v}}_r\\ \tilde{\mathbf{v}}_c\\ \mathbf{v}_1\\ \mathbf{w}_1\end{pmatrix}=\lambda\begin{bmatrix}\acute{\mathbf{M}}_s & \mathbf{0} & \mathbf{0} & \mathbf{0} & \mathbf{0}\\ \mathbf{0} & \acute{\mathbf{M}}_r & \mathbf{0} & \mathbf{0} & \mathbf{0}\\ \mathbf{0} & \mathbf{0} & \acute{\mathbf{M}}_c & \mathbf{0} & \mathbf{0}\\ \mathbf{0} & \mathbf{0} & \mathbf{0} & \frac{p}{2}\mathbf{M}_1 & \mathbf{0}\\ \mathbf{0} & \mathbf{0} & \mathbf{0} & \mathbf{0} & \frac{p}{2}\mathbf{M}_1\end{bmatrix}\begin{pmatrix}\tilde{\mathbf{v}}_s\\ \tilde{\mathbf{v}}_r\\ \tilde{\mathbf{v}}_c\\ \mathbf{v}_1\\ \mathbf{w}_1\end{pmatrix}. \tag{78}$$

The first three rows of Eq. (78) are the same as Eq. (74). The 4th row of Eq. (78) is the same as Eq. (75) because $\sum_{i=2}^{p}\cos\alpha_i$ is non-zero. Similarly, the 5th row of Eq. (78) is the same as Eq. (76). Consequently, Eq. (44) is satisfied for $\mathbf{u}$ satisfying the reduced eigenvalue problem Eq. (78).

The foregoing analysis confirms that the degenerate mode pair $\mathbf{q}_1$ and $\mathbf{q}_2$ defined by Eqs. (34) and (35) each satisfy Eq. (26) with the same eigenvalue. The natural frequency multiplicity of two is also reflected in Eq. (78), which yields 12 degenerate eigenvalues with corresponding eigenvectors $\mathbf{u}_1=(\tilde{\mathbf{v}}_s,\tilde{\mathbf{v}}_r,\tilde{\mathbf{v}}_c,\mathbf{v}_1,\mathbf{w}_1)$ and $\mathbf{u}_2=(\tilde{\mathbf{w}}_s,\tilde{\mathbf{w}}_r,\tilde{\mathbf{w}}_c,\mathbf{w}_1,\mathbf{v}_1)$. This is true because one can exchange the letters $\mathbf{v}$ and $\mathbf{w}$ in Eq. (60) with no change to any subsequent matrices or results. As a result, there are exactly 12 pairs of translational–tilting modes with twice repeated natural frequencies.

3.3.3. Planet modes

The decomposition of the candidate planet mode according to Eqs. (36)–(38) is

$$\mathbf{u}=w_1\mathbf{v}_1,\quad \mathbf{q}^*=(\mathbf{0},\mathbf{0},\mathbf{0},w_2\mathbf{v}_1,\ldots,w_p\mathbf{v}_1), \tag{79}$$

where the zero vectors are 6×1. We specify without loss of generality that $w_1\mathbf{v}_1\neq0$, that is, at least the arbitrarily selected first planet deflects. The modal deflections of other planets are a scalar multiple of the modal deflections of the first planet as given in Eq. (37), although the w_i ($i=1,\ldots,p$) are yet to be determined.

The matrices in Eq. (43) are

$$\mathbf{B}_0=\begin{bmatrix}\mathbf{K}_{s,1}\\ \mathbf{K}_{r,1}\\ \mathbf{K}_{c,1}\end{bmatrix},\quad \mathbf{E}_0=\begin{bmatrix}\mathbf{K}_{s,2} & \ldots & \mathbf{K}_{s,p}\\ \mathbf{K}_{r,2} & \ldots & \mathbf{K}_{r,p}\\ \mathbf{K}_{c,2} & \ldots & \mathbf{K}_{c,p}\end{bmatrix}, \tag{80}$$

where $\mathbf{B}_0$ has dimension 18×6 and $\mathbf{E}_0$ has dimension $18 \times 6(p-1)$. Substitution of Eqs. (79) and (80) into Eq. (43) yields

$$\sum_{i=1}^{p} \mathbf{K}_{h,i} w_i \mathbf{v}_1 = \mathbf{0}, \quad h = s, r, c. \tag{81}$$

Substitution of Eq. (31) into Eq. (81) gives

$$\left(\mathbf{\Lambda}_h \sum_{i=1}^{p} w_i \sin\alpha_i + \mathbf{R}\mathbf{\Lambda}_h \sum_{i=1}^{p} w_i \cos\alpha_i + \mathbf{\Gamma}_h \sum_{i=1}^{p} w_i \right) \mathbf{v}_1 = \mathbf{0}, \tag{82}$$

which is satisfied if

$$\sum_{i=1}^{p} w_i \sin\alpha_i = 0, \quad \sum_{i=1}^{p} w_i \cos\alpha_i = 0, \quad \sum_{i=1}^{p} w_i = 0. \tag{83}$$

Eq. (83) can be solved for $p-3$ solutions for $p \geqslant 4$ [8,17]. Each solution gives a non-trivial set of w_i, $i = 1, \ldots, p$, and this set can be scaled by an arbitrary constant.

The matrices in Eq. (44) are

$$\mathbf{B}_N^{\mathrm{T}} = \mathbf{0}, \quad \mathbf{E}_N = \mathrm{diag}(\mathbf{K}_2, \ldots, \mathbf{K}_p), \quad \mathbf{M}_N = \mathrm{diag}(\mathbf{M}_2, \ldots, \mathbf{M}_p), \tag{84}$$

where $\mathbf{B}_N$ has dimension $6(p-1) \times 6$, and $\mathbf{E}_N$ and $\mathbf{M}_N$ have dimension $6(p-1) \times 6(p-1)$. Substitution of Eqs. (79) and (84) into Eq. (44) gives $\mathbf{K}_i w_i \mathbf{v}_1 = \lambda \mathbf{M}_i w_i \mathbf{v}_1$, $i = 2, \ldots, p$. With use of Eq. (30) and $w_i \neq 0$ for some i, these equations reduce to

$$\mathbf{K}_1 \mathbf{v}_1 = \lambda \mathbf{M}_1 \mathbf{v}_1. \tag{85}$$

We now show that this equation is satisfied by the reduced eigenvalue problem Eq. (40).

Considering Eq. (40), the matrices are given by $\mathbf{A} = \mathbf{K}_1$, $\mathbf{M}_u = \mathbf{M}_1$, and $\mathbf{B}^{\mathrm{T}}\mathbf{Y} = \mathbf{0}$. With $\mathbf{u} = w_1 \mathbf{v}_1$ Eq. (40) becomes

$$\mathbf{K}_1 w_1 \mathbf{v}_1 = \lambda \mathbf{M}_1 w_1 \mathbf{v}_1. \tag{86}$$

Eq. (85) is satisfied for $\mathbf{v}_1$ determined from Eq. (86) and $w_1 \neq 0$. Thus, both Eqs. (40) and (44) are satisfied. Eq. (43) is satisfied by solution of Eq. (83) for the $p-3$ sets of w_i.

Thus, every mode of the form Eq. (79), defined by Eqs. (36) and (37) constructed from $\mathbf{v}_1$ and a set of w_i, satisfies the full eigenvalue problem Eq. (26). The reduced 6×6 eigenvalue problem in Eq. (86) yields six planet mode eigenvalues regardless of the number of planets. For each of the six eigensolution pairs $(\lambda, \mathbf{v}_1)$ one can construct $p-3$ ($p \geqslant 4$) eigenvectors of the full system using the solution sets for the w_i from Eq. (83). Hence, each of the six planet mode natural frequencies has multiplicity $p-3$. There are no planet modes if there are less than four planets because no set of w_i satisfying Eq. (83) can be found.

3.4. Discussion

A helical planetary gear with p equally spaced planets and six degrees of freedom per component has $18 + 6p$ degrees of freedom. There are 12 rotational–axial modes with distinct natural frequencies; there are 24 translational–tilting modes (i.e., 12 degenerate mode pairs with natural frequency multiplicity two); there are six planet modes each with natural frequency multiplicity $p-3$ (i.e., $6(p-3)$ modes) provided $p \geqslant 4$. Thus, all $18 + 6p$ vibration modes have been accounted for. No other mode type is possible.

The only restrictions that the proof needs are the tuned system assumption and equal planet spacing. These restrictions are confined to the plane of the planetary gear. Parameter variations that do not disturb these stipulations have no effect on the properties of the vibration modes. There are no restrictions on the parameters that define the system in the axial direction. Therefore, contrary to intuition, the described mode types hold for configurations that are not symmetric about the plane of the gears, such as:

1. The bearings at opposite ends of a given gear-shaft body have different stiffness properties. An example is tapered roller bearings at one end and spherical roller bearings at the other end.

2. The bearings on a given gear-shaft body are at different distances from the gear plane; both bearings are on the same side of the gear plane; or, there is only one bearing. An example of such a configuration would be overhung gears and/or carrier.
3. The mass centers of the various gear-shaft bodies are at different axial positions.
4. The contact pattern is off-centered at the gear meshes. This may be due to, for example, lead modifications and deflection of the system under load. Note, however, that the sun–planet contact patterns must be the same at each planet (and the same for the ring–planet meshes).

These four items destroy symmetry about the gear plane, but the modal properties hold for these configurations and any combination thereof.

4. Conclusions

We prove that there are exactly three types of vibration modes of any tuned single-stage helical planetary gear system with equally spaced planets. The helical planetary gear system is represented by a three-dimensional lumped-parameter model that allows for six degrees of freedom per gear-shaft body supported by bearings at arbitrary axial positions. All vibration modes belong to one of these three types, described below:

1. Rotational–axial modes: The central members rotate and move axially but do not tilt or translate. The modal deflection of the planets are identical. There are 12 rotational–axial modes with distinct natural frequencies.
2. Translational–tilting modes: The central members tilt and translate in-plane but do not rotate or move axially. The modal deflections of all planets are related to one another according to Eq. (35). There are 12 pairs of degenerate translational–tilting modes with natural frequency multiplicity two.
3. Planet modes: Only the planets have modal deflection. Each planet's modal deflection is a known scalar multiple of any other planet's modal deflection. The central members do not move. There are six planet mode sets, where each set consists of $p-3$ degenerate (for $p>4$) modes having the same natural frequency. Planet modes exist only for systems with four or more planets ($p\geqslant 4$).

This classification of the vibration modes persists for systems that are not symmetric about the plane of the planetary gear because the proof is valid for arbitrary values of all parameters that lead to such asymmetry.

Appendix A. System matrices

For all matrices in the appendix, all unspecified elements are zero.

All sub-matrices in Eqs. (87)–(98) are associated with a particular mesh. Subscript s denotes the sun gear; for sub-matrices with the subscript s, $j=1,3,\ldots,2p-1$ indicates the particular sun–planet mesh. Similarly, for sub-matrices with the subscript r, $j=2,4,\ldots,2p$ indicates the particular ring–planet mesh.

$$\Upsilon_s^{(1,3)}=\Upsilon_s^{(3,1)}=k_j r_s D_1(j)\cos\psi,\quad \Upsilon_s^{(2,3)}=\Upsilon_s^{(3,2)}=k_j r_s^2\sin\psi\cos\psi,$$

$$\Upsilon_s^{(3,5)}=\Upsilon_s^{(5,3)}=k_j r_s\cos^2\psi,\quad \Upsilon_s^{(1,6)}=\Upsilon_s^{(6,1)}=-k_j D_1(j)\sin\psi,$$

$$\Upsilon_s^{(2,6)}=\Upsilon_s^{(6,2)}=-k_j r_s\sin^2\psi. \tag{87}$$

$$\Theta_s^{(1,1)}=\kappa_j+k_j D_1(j)^2,\quad \Theta_s^{(1,2)}=\Theta_s^{(2,1)}=k_j D_1(j) r_s\sin\psi,$$

$$\Theta_s^{(2,2)}=k_j r_s\sin^2\psi,\quad \Theta_s^{(5,5)}=k_j\cos^2\psi,$$

$$\Theta_s^{(1,5)}=\Theta_s^{(5,1)}=k_j D_1(j)\cos\psi,\quad \Theta_s^{(2,5)}=\Theta_s^{(5,2)}=k_j r_s\sin\psi\cos\psi. \tag{88}$$

$$\Xi_s^{(1,1)}=2k_j D_1(j) r_s\sin\psi,\quad \Xi_s^{(1,2)}=\Xi_s^{(2,1)}=k_j[r_s^2\sin^2\psi-D_1(j)^2]-\kappa_j,$$

$$\Xi_s^{(1,4)} = \Xi_s^{(4,1)} = k_j \cos\psi D_1(j), \quad \Xi_s^{(1,5)} = \Xi_s^{(5,1)} = k_j r_s \cos\psi \sin\psi,$$

$$\Xi_s^{(2,2)} = -2k_j D_1(j) r_s \sin\psi, \quad \Xi_s^{(2,4)} = \Xi_s^{(4,2)} = k_j r_s \cos\psi \sin\psi,$$

$$\Xi_s^{(2,5)} = \Xi_s^{(5,2)} = -k_j \cos\psi D_1(j), \quad \Xi_s^{(4,5)} = \Xi_s^{(5,4)} = k_j \cos^2\psi. \tag{89}$$

$$\Psi_s^{(1,1)} = k_s^A D_{17}^2 + k_s^B D_{18}^2 + \kappa_s^A + \kappa_s^B, \quad \Psi_s^{(1,5)} = \Psi_s^{(5,1)} = -k_s^A D_{17} - k_s^B D_{18},$$

$$\Psi_s^{(2,2)} = k_s^A D_{17}^2 + k_s^B D_{18}^2 + \kappa_s^A + \kappa_s^B, \quad \Psi_s^{(2,4)} = \Psi_s^{(4,2)} = k_s^A D_{17} + k_s^B D_{18},$$

$$\Psi_s^{(3,3)} = \kappa_s^{Az} + \kappa_s^{Bz} + k_j r_s^2 \cos^2\psi, \quad \Psi_s^{(3,6)} = -k_j r_s \cos\psi \sin\psi, \quad \Psi_s^{(4,4)} = k_s^A + k_s^B,$$

$$\Psi_s^{(5,5)} = k_s^A + k_s^B, \quad \Psi_s^{(6,6)} = k_s^{Az} + k_s^{Bz} + k_j \sin^2\psi. \tag{90}$$

$$\Lambda_s^{(1,1)} = k_j D_1(j) r_p \sin\psi, \quad \Lambda_s^{(1,2)} = k_j D_1(j) D_2(j) + \kappa_j, \quad \Lambda_s^{(1,3)} = k_j D_1(j) r_p \cos\psi,$$

$$\Lambda_s^{(1,4)} = -k_j D_1(j) \cos\psi, \quad \Lambda_s^{(1,6)} = k_j D_1(j) \sin\psi, \quad \Lambda_s^{(2,1)} = k_j r_s r_p \sin^2\psi,$$

$$\Lambda_s^{(2,2)} = k_j r_s \sin\psi D_2(j), \quad \Lambda_s^{(2,3)} = k_j r_s r_p \sin\psi \cos\psi, \quad \Lambda_s^{(2,4)} = -k_j r_s \sin\psi \cos\psi,$$

$$\Lambda_s^{(2,6)} = k_j r_s \sin^2\psi, \quad \Lambda_s^{(5,1)} = k_j r_p \cos\psi \sin\psi, \quad \Lambda_s^{(5,2)} = k_j \cos\psi D_2(j),$$

$$\Lambda_s^{(5,3)} = k_j r_p \cos^2\psi, \quad \Lambda_s^{(5,4)} = -k_j \cos^2\psi, \quad \Lambda_s^{(5,6)} = k_j \sin\psi \cos\psi. \tag{91}$$

$$\Gamma_s^{(3,1)} = k_j r_s r_p \cos\psi \sin\psi, \quad \Gamma_s^{(3,2)} = k_j r_s \cos\psi D_2(j), \quad \Gamma_s^{(3,3)} = k_j r_p r_s \cos^2\psi,$$

$$\Gamma_s^{(3,4)} = -k_j r_s \cos^2\psi, \quad \Gamma_s^{(3,6)} = k_j r_s \cos\psi \sin\psi, \quad \Gamma_s^{(6,1)} = -k_j r_p \sin^2\psi,$$

$$\Gamma_s^{(6,2)} = -k_j \sin\psi D_2(j), \quad \Gamma_s^{(6,3)} = -k_j r_p \sin\psi \cos\psi, \quad \Gamma_s^{(6,4)} = k_j \sin\psi \cos\psi,$$

$$\Gamma_s^{(6,6)} = -k_j \sin^2\psi, \tag{92}$$

where $j = 1, 3, \ldots, 2p-1$ for all matrices related to the sun.

$$\Upsilon_r^{(1,3)} = \Upsilon_r^{(3,1)} = k_j r_r D_3(j) \cos\psi, \quad \Upsilon_r^{(1,6)} = \Upsilon_r^{(6,1)} = k_j D_3(j) \sin\psi,$$

$$\Upsilon_r^{(2,3)} = \Upsilon_r^{(3,1)} = k_j r_r D_4(j) \cos\psi, \quad \Upsilon_r^{(2,6)} = \Upsilon_r^{(6,2)} = k_j D_4(j) \sin\psi,$$

$$\Upsilon_r^{(3,4)} = \Upsilon_r^{(4,3)} = k_j r_r D_5 \cos\psi, \quad \Upsilon_r^{(3,5)} = \Upsilon_r^{(5,3)} = k_j r_r D_6 \cos\psi,$$

$$\Upsilon_r^{(4,6)} = \Upsilon_r^{(6,4)} = k_j D_5 \sin\psi, \quad \Upsilon_r^{(5,6)} = \Upsilon_r^{(6,5)} = k_j D_6 \sin\psi. \tag{93}$$

$$\Theta_r^{(1,1)} = \kappa_j D_9^2 + k_j D_3(j)^2, \quad \Theta_r^{(1,2)} = \Theta_r^{(2,1)} = \kappa_j D_9 D_{10} + k_j D_3(j) D_4(j),$$

$$\Theta_r^{(1,4)} = \Theta_r^{(4,1)} = k_j D_3(j) D_5, \quad \Theta_r^{(1,5)} = \Theta_r^{(5,1)} = k_j D_3(j) D_6,$$

$$\Theta_r^{(2,2)} = \kappa_j D_{10}^2 + k_j D_4(j)^2, \quad \Theta_r^{(2,4)} = \Theta_r^{(4,2)} = k_j D_4(j) D_5,$$

$$\Theta_r^{(2,5)} = \Theta_r^{(5,2)} = k_j D_4(j) D_6, \quad \Theta_r^{(4,4)} = k_j D_5^2,$$

$$\Theta_r^{(4,5)} = \Theta_r^{(5,4)} = k_j D_5 D_6, \quad \Theta_r^{(5,5)} = k_j D_6^2. \tag{94}$$

$$\Xi_r^{(1,1)} = 2\kappa_j D_9 D_{10} + 2k_j D_3(j) D_4(j),$$

$$\Xi_r^{(1,2)} = \Xi_r^{(2,1)} = k_j[D_4(j)^2 - D_3(j)^2] + \kappa_j(D_{10}^2 - D_9^2),$$

$$\Xi_r^{(1,4)} = \Xi_r^{(4,1)} = k_j[D_3(j)D_6 + D_4(j)D_5],$$

$$\Xi_r^{(1,5)} = \Xi_r^{(5,1)} = k_j[D_4(j)D_6 - D_3(j)D_5],$$

$$\Xi_r^{(2,2)} = -2\kappa_j D_9 D_{10} - 2k_j D_3(j)D_4(j),$$

$$\Xi_r^{(2,4)} = \Xi_r^{(4,2)} = k_j[D_4(j)D_6 - D_3(j)D_5], \quad \Xi_r^{(4,4)} = 2k_j D_5 D_6,$$

$$\Xi_r^{(2,5)} = \Xi_r^{(5,2)} = -k_j[D_3(j)D_6 + D_4(j)D_5],$$

$$\Xi_r^{(4,5)} = \Xi_r^{(5,4)} = k_j(D_6^2 - D_5^2), \quad \Xi_r^{(5,5)} = -2k_j D_5 D_6. \tag{95}$$

$$\Psi_r^{(1,1)} = k_r^A D_{19}^2 + k_r^B D_{20}^2 + \kappa_r^A + \kappa_r^B, \quad \Psi_r^{(1,5)} = \Psi_r^{(5,1)} = -k_r^A D_{19} - k_r^B D_{20},$$

$$\Psi_r^{(2,2)} = k_r^A D_{19}^2 + k_r^B D_{20}^2 + \kappa_r^A + \kappa_r^B, \quad \Psi_r^{(2,4)} = \Psi_r^{(4,2)} = k_r^A D_{19} + k_r^B D_{20},$$

$$\Psi_r^{(3,3)} = \kappa_r^{Az} + \kappa_r^{Bz} + k_j r_r^2 \cos^2\psi, \quad \Psi_r^{(3,6)} = \Psi_r^{(6,3)} = k_j r_r \cos\psi \sin\psi,$$

$$\Psi_r^{(4,4)} = k_r^A + k_r^B, \quad \Psi_r^{(5,5)} = k_r^A + k_r^B, \quad \Psi_r^{(6,6)} = k_r^{Az} + k_r^{Bz} + k_j \sin^2\psi. \tag{96}$$

$$\Lambda_r^{(1,1)} = k_j D_3(j)D_7(j) - \kappa_j D_9 D_{10}, \quad \Lambda_r^{(1,2)} = k_j D_3(j)D_8(j) + \kappa_j D_9^2,$$

$$\Lambda_r^{(1,4)} = -k_j D_3(j)D_6, \quad \Lambda_r^{(1,5)} = k_j D_3(j)D_5, \quad \Lambda_r^{(1,6)} = -k_j D_3(j)\sin\psi,$$

$$\Lambda_r^{(1,3)} = -k_j r_p D_3(j)\cos\psi, \quad \Lambda_r^{(2,3)} = -k_j r_p D_4(j)\cos\psi,$$

$$\Lambda_r^{(2,1)} = k_j D_4(j)D_7(j) - \kappa_j D_{10}^2, \quad \Lambda_r^{(2,2)} = k_j D_4(j)D_8(j) + \kappa_j D_9 D_{10},$$

$$\Lambda_r^{(2,4)} = -k_j D_4(j)D_6, \quad \Lambda_r^{(2,5)} = k_j D_4(j)D_5, \quad \Lambda_r^{(2,6)} = -k_j \sin\psi D_4(j),$$

$$\Lambda_r^{(4,1)} = k_j D_5 D_7(j), \quad \Lambda_r^{(4,2)} = k_j D_5 D_8(j), \quad \Lambda_r^{(4,3)} = -k_j D_5 r_p \cos\psi,$$

$$\Lambda_r^{(4,4)} = -k_j D_5 D_6, \quad \Lambda_r^{(4,5)} = k_j D_5^2, \quad \Lambda_r^{(4,6)} = -k_j D_5 \sin\psi,$$

$$\Lambda_r^{(5,1)} = k_j D_6 D_7(j), \quad \Lambda_r^{(5,2)} = k_j D_6 D_8(j), \quad \Lambda_r^{(5,3)} = -k_j r_p D_6 \cos\psi,$$

$$\Lambda_r^{(5,4)} = -k_j D_6^2, \quad \Lambda_r^{(5,5)} = k_j D_5 D_6, \quad \Lambda_r^{(5,6)} = -k_j \sin\psi D_6. \tag{97}$$

$$\Gamma_r^{(3,1)} = k_j r_r \cos\psi D_7(j), \quad \Gamma_r^{(3,2)} = k_j r_r \cos\psi D_8(j), \quad \Gamma_r^{(3,3)} = -k_j r_r r_p \cos^2\psi,$$

$$\Gamma_r^{(3,4)} = -k_j r_r D_6 \cos\psi, \quad \Gamma_r^{(3,5)} = k_j r_r D_5 \cos\psi, \quad \Gamma_r^{(3,6)} = -k_j r_r \sin\psi\cos\psi,$$

$$\Gamma_r^{(6,1)} = k_j \sin\psi D_7(j), \quad \Gamma_r^{(6,2)} = k_j \sin\psi D_8(j), \quad \Gamma_r^{(6,3)} = -k_j r_p \sin\psi\cos\psi,$$

$$\Gamma_r^{(6,4)} = -k_j \sin\psi D_6, \quad \Gamma_r^{(6,5)} = k_j \sin\psi D_5, \quad \Gamma_r^{(6,6)} = -k_j \sin^2\psi, \tag{98}$$

where $j = 2, 4, \ldots, 2p$ for all matrices related to the ring.

$$\Upsilon_c^{(1,3)} = \Upsilon_c^{(3,1)} = -D_{13}(k_p^A D_{11} + k_p^B D_{15}), \quad \Upsilon_c^{(1,6)} = \Upsilon_c^{(6,1)} = -D_{12}(k_p^{Az} + k_p^{Bz}),$$

$$\Upsilon_c^{(2,3)} = \Upsilon_c^{(3,2)} = D_{12}(k_p^A D_{11} + k_p^B D_{15}), \quad \Upsilon_c^{(2,6)} = \Upsilon_c^{(6,2)} = -D_{13}(k_p^{Az} + k_p^{Bz}),$$

$$\Upsilon_c^{(3,4)} = \Upsilon_c^{(4,3)} = D_{12}(k_p^A + k_p^B), \quad \Upsilon_c^{(3,5)} = \Upsilon_c^{(5,3)} = D_{13}(k_p^A + k_p^B). \tag{99}$$

$$\Theta_c^{(1,1)} = k_p^A D_{11}^2 + k_p^B D_{15}^2 + D_{12}^2(k_p^{Az} + k_p^{Bz}) + \kappa_p^A + \kappa_p^B,$$

$$\Theta_c^{(1,2)} = \Theta_c^{(2,1)} = D_{12}D_{13}(k_p^{Az} + k_p^{Bz}),$$

$$\Theta_c^{(1,5)} = \Theta_c^{(5,1)} = -k_p^A D_{11} - k_p^B D_{15},$$

$$\Theta_c^{(2,2)} = k_p^A D_{11}^2 + k_p^B D_{15}^2 + D_{13}^2(k_p^{Az} + k_p^{Bz}) + \kappa_p^A + \kappa_p^B,$$

$$\Theta_c^{(2,4)} = \Theta_c^{(4,2)} = k_p^A D_{11} + k_p^B D_{15}, \quad \Theta_c^{(4,4)} = k_p^A + k_p^B,$$

$$\Theta_c^{(5,5)} = k_p^A + k_p^B. \tag{100}$$

$$\Xi_c^{(1,1)} = 2D_{12}D_{13}(k_p^{Az} + k_p^{Bz}), \quad \Xi_c^{(2,2)} = -2D_{12}D_{13}(k_p^{Az} + k_p^{Bz}),$$

$$\Xi_c^{(1,2)} = \Xi_c^{(2,1)} = (D_{13}^2 - D_{12}^2)(k_p^{Az} + k_p^{Bz}). \tag{101}$$

$$\Psi_c^{(1,1)} = k_c^A D_{21}^2 + k_c^B D_{22}^2 + \kappa_c^A + \kappa_c^B, \quad \Psi_c^{(1,5)} = \Psi_c^{(5,1)} = -k_c^A D_{21} - k_c^B D_{22},$$

$$\Psi_c^{(2,2)} = k_c^A D_{21}^2 + k_c^B D_{22}^2 + \kappa_c^A + \kappa_c^B, \quad \Psi_c^{(2,4)} = \Psi_c^{(4,2)} = k_c^A D_{21} + k_c^B D_{22},$$

$$\Psi_c^{(3,3)} = \kappa_c^{Az} + \kappa_c^{Bz} + \kappa_p^{Az} + \kappa_p^{Bz} + (D_{13}^2 + D_{12}^2)(k_p^A + k_p^B),$$

$$\Psi_c^{(4,4)} = k_c^A + k_c^B, \quad \Psi_c^{(5,5)} = k_c^A + k_c^B, \quad \Psi_c^{(6,6)} = k_c^{Az} + k_c^{Bz} + k_p^{Az} + k_p^{Bz}. \tag{102}$$

$$\Lambda_c^{(1,2)} = k_p^A D_{11}D_{14} + k_p^B D_{15}D_{16} + \kappa_p^A + \kappa_p^B,$$

$$\Lambda_c^{(2,1)} = -k_p^A D_{11}D_{14} - k_p^B D_{15}D_{16} - \kappa_p^A - \kappa_p^B,$$

$$\Lambda_c^{(4,1)} = -k_p^A D_{14} - k_p^B D_{16}, \quad \Lambda_c^{(4,5)} = k_p^A + k_p^B,$$

$$\Lambda_c^{(5,2)} = -k_p^A D_{14} - k_p^B D_{16}, \quad \Lambda_c^{(5,4)} = -k_p^A - k_p^B,$$

$$\Lambda_c^{(1,4)} = k_p^A D_{11} + k_p^B D_{15}, \quad \Lambda_c^{(2,5)} = k_p^A D_{11} + k_p^B D_{15},$$

$$\Lambda_c^{(1,6)} = D_{12}(k_p^{Az} + k_p^{Bz}), \quad \Lambda_c^{(2,6)} = D_{13}(k_p^{Az} + k_p^{Bz}). \tag{103}$$

$$\Gamma_c^{(3,1)} = -D_{12}(k_p^A D_{14} + k_p^B D_{16}), \quad \Gamma_c^{(3,2)} = -D_{13}(k_p^A D_{14} + k_p^B D_{16}),$$

$$\Gamma_c^{(3,3)} = -\kappa_p^{Az} - \kappa_p^{Bz}, \quad \Gamma_c^{(3,4)} = -D_{13}(k_p^A + k_p^B),$$

$$\Gamma_c^{(3,5)} = D_{12}(k_p^A + k_p^B), \quad \Gamma_c^{(6,6)} = -k_p^{Az} - k_p^{Bz}. \tag{104}$$

Eq. (105) relates to planet $i \in \{1, 2, \ldots, p\}$. The quantity $2i-1$ indicates the sun–planet mesh, and $2i$ indicates the ring-planet mesh.

$$\mathbf{K}_i^{(1,1)} = k_{2i-1} r_p^2 \sin^2\psi + k_{2i} D_7 (2i)^2 + \kappa_{2i} D_{10}^2 + k_p^A D_{14}^2 + k_p^B D_{16}^2 + \kappa_p^A + \kappa_p^B,$$

$$\mathbf{K}_i^{(1,2)} = \mathbf{K}_i^{(2,1)} = k_{2i-1} D_2 (2i-1) r_p \sin\psi + k_{2i} D_7 (2i) D_8 (2i) - \kappa_{2i} D_9 D_{10},$$

$$\mathbf{K}_i^{(1,3)} = \mathbf{K}_i^{(3,1)} = [k_{2i-1} r_p \sin\psi - k_{2i} D_7(2i)] r_p \cos\psi,$$

$$\mathbf{K}_i^{(1,5)} = \mathbf{K}_i^{(5,1)} = k_{2i} D_7(2i) D_5 - k_p^A D_{14} - k_p^B D_{16},$$

$$\mathbf{K}_i^{(1,4)} = \mathbf{K}_i^{(4,1)} = -k_{2i-1} r_p \sin\psi\cos\psi - k_{2i} D_7(2i) D_6,$$

$$\mathbf{K}_i^{(1,6)} = \mathbf{K}_i^{(6,1)} = k_{2i-1} r_p \sin^2\psi - k_{2i} D_7(2i)\sin\psi,$$

$$\mathbf{K}_i^{(2,2)} = k_{2i-1} D_2(2i-1)^2 + k_{2i} D_8(2i)^2 + \kappa_{2i-1} + \kappa_{2i} D_9^2 + k_p^A D_{14}^2 + k_p^B D_{16}^2 + \kappa_p^A + \kappa_p^B,$$

$$\mathbf{K}_i^{(2,3)} = \mathbf{K}_i^{(3,2)} = [k_{2i-1} D_2(2i-1) - k_{2i} D_8(2i)] r_p \cos\psi,$$

$$\mathbf{K}_i^{(2,4)} = \mathbf{K}_i^{(4,2)} = -k_{2i-1} D_2(2i-1)\cos\psi - k_{2i} D_8(2i) D_6 + k_p^A D_{14} + k_p^B D_{16},$$

$$\mathbf{K}_i^{(2,5)} = \mathbf{K}_i^{(5,2)} = k_{2i} D_5 D_8(2i),$$

$$\mathbf{K}_i^{(2,6)} = \mathbf{K}_i^{(6,2)} = k_{2i-1} D_2(2i-1)\sin\psi - k_{2i} D_8(2i)\sin\psi,$$

$$\mathbf{K}_i^{(3,3)} = (k_{2i-1} + k_{2i}) r_p^2 \cos^2\psi + \kappa_p^{Az} + \kappa_p^{Bz},$$

$$\mathbf{K}_i^{(3,4)} = \mathbf{K}_i^{(4,3)} = (k_{2i} D_6 - k_{2i-1}\cos\psi) r_p \cos\psi,$$

$$\mathbf{K}_i^{(3,5)} = \mathbf{K}_i^{(5,3)} = -k_{2i} D_5 r_p \cos\psi,$$

$$\mathbf{K}_i^{(3,6)} = \mathbf{K}_i^{(6,3)} = (k_{2i-1} + k_{2i}) r_p \sin\psi\cos\psi,$$

$$\mathbf{K}_i^{(4,4)} = k_{2i-1}\cos^2\psi + k_{2i} D_6^2 + k_p^A + k_p^B, \quad \mathbf{K}_i^{(4,5)} = \mathbf{K}_i^{(5,4)} = -k_{2i} D_5 D_6,$$

$$\mathbf{K}_i^{(4,6)} = \mathbf{K}_i^{(6,4)} = -(k_{2i-1}\cos\psi - k_{2i} D_6)\sin\psi,$$

$$\mathbf{K}_i^{(5,5)} = k_{2i} D_5^2 + k_p^A + k_p^B, \quad \mathbf{K}_i^{(5,6)} = \mathbf{K}_i^{(6,5)} = -k_{2i} D_5 \sin\psi,$$

$$\mathbf{K}_i^{(6,6)} = (k_{2i-1} + k_{2i})\sin^2\psi + k_p^{Az} + k_p^{Bz}. \tag{105}$$

In the quantities below, $j \in \{1, 2, \ldots, 2p\}$ denotes one of the $2p$ tooth meshes:

$$D_1(j) = (e_s - c_j)\cos\psi - r_s \sin\psi \tan\Phi_{\mathrm{sp}},$$

$$D_2(j) = (e_p - c_j)\cos\psi + r_p \sin\psi \tan\Phi_{\mathrm{sp}},$$

$$D_3(j) = \cos(\Phi_{\mathrm{sp}} + \Phi_{\mathrm{rp}})[(e_r - c_j)\cos\psi - r_r \sin\psi \tan\Phi_{\mathrm{rp}}] + r_r \sin\psi \sin(\Phi_{\mathrm{sp}} + \Phi_{\mathrm{rp}}),$$

$$D_4(j) = \sin(\Phi_{\mathrm{sp}} + \Phi_{\mathrm{rp}})[(e_r - c_j)\cos\psi - r_r \sin\psi \tan\Phi_{\mathrm{rp}}] - r_r \sin\psi \cos(\Phi_{\mathrm{sp}} + \Phi_{\mathrm{rp}}),$$

$$D_5 = -\cos\psi \sin(\Phi_{\mathrm{sp}} + \Phi_{\mathrm{rp}}), \quad D_6 = \cos\psi\cos(\Phi_{\mathrm{sp}} + \Phi_{\mathrm{rp}}),$$

$$D_7(j) = \sin(\Phi_{\mathrm{sp}} + \Phi_{\mathrm{rp}})[(c_j - e_p)\cos\psi + r_p \tan\Phi_{\mathrm{rp}} \sin\psi] + r_p \sin\psi\cos(\Phi_{\mathrm{sp}} + \Phi_{\mathrm{rp}}),$$

$$D_8(j) = \cos(\Phi_{\mathrm{sp}} + \Phi_{\mathrm{rp}})[(e_p - c_j)\cos\psi - r_p \tan\Phi_{\mathrm{rp}} \sin\psi] + r_p \sin\psi \sin(\Phi_{\mathrm{sp}} + \Phi_{\mathrm{rp}}),$$

$$D_9 = -\cos(\Phi_{\mathrm{sp}} + \Phi_{\mathrm{rp}}), \quad D_{10} = -\sin(\Phi_{\mathrm{sp}} + \Phi_{\mathrm{rp}}),$$

$$D_{11} = -L_p^A - e_s, \quad D_{12} = -\tan\Phi_{\mathrm{sp}}(r_s + r_p), \quad D_{13} = r_s + r_p, \quad D_{14} = -L_p^A - e_p,$$

$$D_{15} = L_p^B - e_s, \quad D_{16} = L_p^B - e_p, \quad D_{17} = -L_s^A - e_s, \quad D_{18} = L_s^B - e_s,$$

$$D_{19} = -L_r^A - e_r, \quad D_{20} = L_r^B - e_r, \quad D_{21} = -L_c^A - e_c, \quad D_{22} = L_c^B - e_c.$$

References

[1] F. Cunliffe, J.D. Smith, D.B. Welbourn, Dynamic tooth loads in epicyclic gears, *Journal of Engineering for Industry* 5 (95) (1974) 578–584.

[2] D.L. Seager, Conditions for the neutralization of excitation by the teeth in epicyclic gearing, *Journal of Mechanical Engineering Science* 17 (5) (1975) 293–298.
[3] M. Botman, Epicyclic gear vibrations, *Journal of Engineering for Industry* (1976) 811–815.
[4] R. August, R. Kasuba, Torsional vibrations and dynamic loads in a basic planetary gear system, *Journal of Vibration, Acoustics, Stress, and Reliability in Design* 108 (3) (1986) 348–353.
[5] J. Lin, R.G. Parker, Analytical characterization of the unique properties of planetary gear free vibration, *Journal of Vibration and Acoustics* 121 (3) (1999) 316–321.
[6] J. Lin, R.G. Parker, Structured vibration characteristics of planetary gears with unequally spaced planets, *Journal of Sound and Vibration* 233 (5) (2000) 921–928.
[7] D.R. Kiracofe, R.G. Parker, Structured vibration modes of general compound planetary gear systems, *Journal of Vibration and Acoustics* 129 (1) (2007) 1–16.
[8] X. Wu, R.G. Parker, Modal properties of planetary gears with an elastic continuum ring gear, *Journal of Applied Mechanics* 75 (3) (2008) 1–10.
[9] J. Lin, R.G. Parker, Mesh phasing relationships in planetary and epicyclic gears, *Journal of Mechanical Design* 126 (2004) 365–370.
[10] R.G. Schlegel, K.C. Mard, Transmission noise control approaches in helicopter design, in: *ASME Design Engineering Conference*, No. 67-DE-58, New York, NY, 1967.
[11] J. Lin, R.G. Parker, Sensitivity of planetary gear natural frequencies and vibration modes to model parameters, *Journal of Sound and Vibration* 228 (1) (1999) 109–128.
[12] Y. Guo, R.G. Parker, Sensitivity of general compound planetary gear natural frequencies and vibration modes to modal parameters, *Journal of Vibration and Acoustics*, submitted for publication.
[13] T. Hidaka, Y. Terauchi, K. Nagamura, Dynamic behavior of planetary gear (6th report, influence of meshing-phase), *Bulletin of JSME* 22 (169) (1979) 1026–1033.
[14] A. Kahraman, Planetary gear train dynamics, *Journal of Mechanical Design* 116 (3) (1993) 713–720.
[15] A. Kahraman, G.W. Blankenship, Planet mesh phasing in epicyclic gear sets, in: *International Gearing Conference*, Newcastle, UK, 1994, pp. 99–104.
[16] R.G. Parker, A physical explanation for the effectiveness of planet phasing to suppress planetary gear vibration, *Journal of Sound and Vibration* 236 (2000) 561–573.
[17] V.K. Ambarisha, R.G. Parker, Suppression of planet mode response in planetary gear dynamics through mesh phasing, *Journal of Vibration and Acoustics* 128 (2) (2006) 133–142.
[18] A. Saada, P. Velex, An extended model for the analysis of the dynamic behavior of planetary trains, *Journal of Mechanical Design* 117 (2) (1995) 241–247.
[19] V. Abousleiman, P. Velex, A hybrid 3d finite element/lumped parameter model for quasi-static and dynamic analyses of planetary/epicyclic gear sets, *Mechanism and Machine Theory* 41 (6) (2006) 725–748.
[20] V.K. Ambarisha, R.G. Parker, Nonlinear dynamics of planetary gears using analytical and finite element models, *Journal of Sound and Vibration* 302 (3) (2007) 577–595.
[21] R.G. Parker, V. Agashe, S.M. Vijayakar, Dynamic response of a planetary gear system using a finite element/contact mechanics model, *Journal of Mechanical Design* 122 (3) (2000) 304–310.
[22] P. Velex, M. Maatar, A mathematical model for analyzing the influence of shape deviations and mounting errors on gear dynamic behavior, *Journal of Sound and Vibration* 191 (5) (1996) 629–660.
[23] I.S. Gradshteyn, I.M. Ryzhik, *Table of Integrals, Series, and Products*, Academic Press, New York, 1980.